

PRISMLAYERS: OPEN DATA FOR HIGH-QUALITY MULTI-LAYER TRANSPARENT IMAGE GENERATIVE MODELS

Anonymous authors

Paper under double-blind review

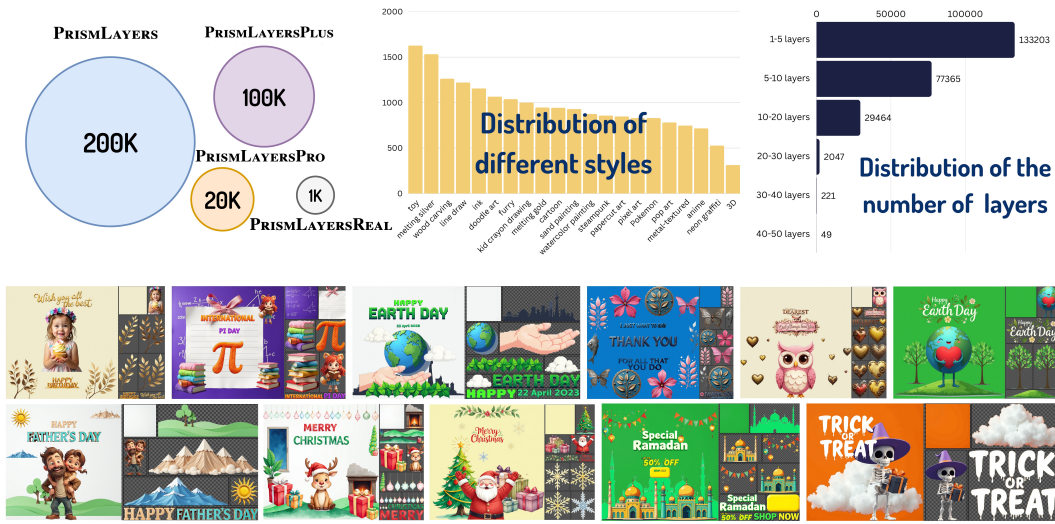


Figure 1: Illustration of key statistics from PRISMLAYERS (number of layers) and PRISMLAYERSPRO (different styles), along with representative high-quality synthetic multi-layer transparent images from PRISMLAYERSPRO.

ABSTRACT

Generating high-quality, multi-layer transparent images from text prompts can unlock a new level of creative control, allowing users to edit each layer as effortlessly as editing text outputs from LLMs. However, the development of multi-layer generative models lags behind that of conventional text-to-image models due to the absence of a large, high-quality corpus of multi-layer transparent data. We address this fundamental challenge by: (i) releasing four open, ultra-high-fidelity datasets—PRISMLAYERS, PRISMLAYERSPLUS, PRISMLAYERSPRO, and PRISMLAYERSREAL—consisting of 200K, 100K, 20K, and 1K multi-layer transparent images with accurate alpha mattes, respectively. (ii) introducing a training-free synthesis pipeline that generates such data on demand using off-the-shelf diffusion models, and (iii) delivering a strong multi-layer generation model, ART+, which matches the aesthetics of modern text-to-image generation models. The key technical contributions include: LayerFLUX, which excels at generating high-quality single transparent layers with accurate alpha mattes, and MultiLayerFLUX, which composes multiple LayerFLUX outputs into complete images, guided by human-annotated semantic layout. To ensure higher quality, we apply a rigorous filtering stage to remove artifacts and semantic mismatches, followed by human selection. Fine-tuning the state-of-the-art ART model on our synthetic PRISMLAYERSPRO yields ART+, which outperforms the original ART in 60% of head-to-head user study comparisons and even matches the visual quality of images generated by the FLUX.1-[dev] model. Our work establishes a solid dataset foundation for multi-layer transparent image generation, enabling research and applications that require precise, editable, and visually compelling layered imagery.

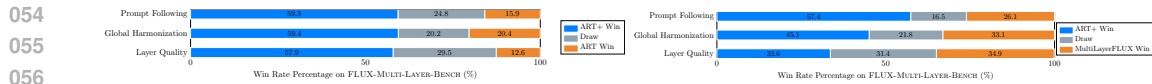


Figure 2: User study results on the effectiveness of PRISMLAYERSPRO. Left: ART+ v.s. ART. Right: ART+ v.s. MultiLayerFLUX. With fine-tuning on PRISMLAYERSPRO, ART+ achieves the best performance.

1 INTRODUCTION

Despite remarkable advances in text-to-image diffusion models, users still face significant challenges in refining outputs to achieve satisfactory results. The difficulty lies in the fact that users cannot precisely articulate their visual requirements before seeing generated images, leading to laborious post-processing workflows. The fundamental issue here is that existing diffusion models are designed to produce single-layer images, lacking the transparent layers and precise alpha mattes required for flexible, layer-wise editing. Modern image editing workflows rely on multi-layered structures for the smooth adjustment of individual elements without causing disruption to the entire composition.

In this paper, we argue for a paradigm shift—from text-to-image generation to text-to-layered-image generation. Such an evolution would empower models to support flexible, layer-wise editing operations that align closely with professional design workflows. The fundamental challenge hindering progress in this area is the lack of high-quality multi-layer image datasets featuring both visually appealing transparency and accurate alpha mattes. Bridging this gap is essential to unlocking the full potential of layered image generation with diffusion models.

Nevertheless, existing literature still relies on the conventional pipeline of fine-tuning generative models on limited, low-quality crawled multi-layer datasets. These datasets have two major drawbacks: (i) aesthetic quality: our empirical analysis shows that the aesthetic scores of crawled multi-layer images are significantly lower than those of RGB images generated by state-of-the-art diffusion models like FLUX.1-[dev]. As a result, we empirically find that fine-tuning on less visually appealing data can degrade the overall aesthetics; (ii) dataset size: the scale of these crawled multi-layer datasets is much smaller than that of conventional RGB image datasets. Consequently, fine-tuning on such datasets becomes less effective as the foundational generative models become increasingly powerful.

This paper leverages off-the-shelf powerful diffusion models to generate high-quality multi-layer transparent images, thereby bypassing the need for fine-tuning on specific datasets. To achieve this goal, this paper makes three key contributions: (i) LayerFLUX: We propose a training-free, single-layer transparent image generation system that utilizes a generate-then-matting scheme. Specifically, our approach leverages diffusion models to generate images with solid-colored backgrounds and uses a state-of-the-art image matting model to extract high-quality alpha masks for salient objects. We have named this system LayerFLUX, as it builds upon the latest diffusion transformer model, FLUX.1-[dev]. (ii) MultiLayerFLUX: We introduce a layout-then-layer scheme that composes multiple high-quality transparent layers generated by LayerFLUX according to a given layout, which can be obtained either from a reference image or generated using an LLM. This modular approach enables precise control over spatial composition while preserving the visual quality and alpha matte of each layer, resulting in our MultiLayerFLUX system. (iii) Transparent Image Preference Scoring Model: We develop a dedicated preference scoring model to assess the visual aesthetics of the generated transparent images. Figure 1 shows the high-quality synthetic multi-layer transparent images generated using MultiLayerFLUX.

To validate our designs, we first compare LayerFLUX with prior transparent image generation methods such as LayerDiffuse Zhang & Agrawala (2024). As shown in Figure 13, user studies on LAYER-BENCH (covering natural objects, sticker/text, and creative layers) confirm clear advantages. Next, we use MultiLayerFLUX to build PRISMLAYERS, a ~200K multi-layer transparent dataset. After filtering, we obtain a 20K high-quality subset (PRISMLAYERSPRO), a 100K loosely filtered set (PRISMLAYERSPLUS), and a 1K photorealistic set (PRISMLAYERSREAL). Fine-tuning ART Pu et al. (2025) on PRISMLAYERSPRO yields ART+, which user studies (Figure 2) prefer in 57–60% of cases for prompt alignment, harmonization, and layer quality. Empirically, ART+ even approaches the quality of holistic single-layer images from FLUX.1-[dev]. These results highlight the critical role of high-quality multi-layer datasets in advancing next-generation transparent image generation, and we expect our open-source dataset to provide a strong foundation for future work.

108
109
110
2 RELATED WORK111
112
113
114
115
116
117
118
119
120
121
122
123
124
125
126
127
128
129
130

Transparent layer generation. The task of transparent image generation has garnered increasing attention due to its high demand in interactive content creation, such as graphic design and presentation slides. Existing efforts can be broadly classified into two categories: (i) *Single-layer transparent image generation*: The representative LayerDiffuse Zhang & Agrawala (2024) introduces both a transparent layer generation model and a background-conditioned variant that produces layers consistent with the background. Text2Layer Zhang et al. (2023) directly trains a text-to-two-layer generation model that converts a text prompt into a foreground layer with a high-quality alpha matte and a corresponding coherent background layer. LayeringDiff Kang et al. (2025) proposes a two-stage approach: first, it generates a composite image using an off-the-shelf generative model, and then it disassembles this image into its foreground and background components via a segmentation or matting model, augmented by a diffusion-based layer separation model that refines the foreground and inpaints the background. (ii) *Multi-layer transparent image generation*: In contrast, LayerDiff Huang et al. (2024) introduces a layer-collaborative diffusion model capable of generating up to four layers from a text prompt. Following this direction, PSDiffusion Huang et al. (2025a) and DreamLayer Huang et al. (2025b) further explore harmonized generation mechanisms, utilizing global layout alignment and attention-based interaction to ensure coherence across multiple layers. ART Pu et al. (2025) employs an anonymous region transformer for variable multi-layer transparent image generation. Unlike the most related MULAN Tudosiu et al. (2024), which uses a top-down approach to decompose a monocular RGB image into a stack of RGBA layers representing the background and isolated instances, our approach adopts a bottom-up scheme. We first generate high-quality transparent layers and subsequently compose them into a unified graphic design. We also show that the visual aesthetic score statistics of the constructed PRISM^LAYERS significantly outperform those of previous datasets.

131
132
133
134
135
136
137
138
139
140
141
142

Graphic design generation. Recently, an increasing number of studies Lin et al. (2024b); Weng et al. (2024); Lin et al. (2024a); Shabani et al. (2024); Kikuchi et al. (2024); Lin et al. (2023); Jia et al. (2023); Inoue et al. (2024); Peng et al. (2025) have shifted their focus from conventional photorealistic image generation to graphic design generation, driven by its substantial business value. One common approach involves generating all image layers simultaneously. For example, COLE Jia et al. (2023) and OpenCOLE Inoue et al. (2024) begin with a brief user prompt and employ multiple LLMs and diffusion models to iteratively generate each element of the final image. In contrast, Graphist Cheng et al. (2024) proposes a hierarchical layout generation system that creates graphic compositions from an unordered set of design elements. In this paper, we focus on building open, high-quality multi-layer transparent image datasets to facilitate future work on closing the gap between multi-layer generation and conventional single-layer text-to-image models. We also discuss the connections between our benchmark and previous multi-layer transparent image generation datasets in Table 1.

143
144
145
3 PRISM^LAYERS: A HIGH-QUALITY MULTI-LAYER TRANSPARENT IMAGE DATASET
146147
148
149
150
151
152
153
We introduce PRISM^LAYERS, a synthetic dataset of $\sim 200K$ multi-layer transparent images, each with a global caption, layer-wise captions, RGB layers, and precise alpha mattes. All samples are filtered via our Transparent Image Preference Score (TIPS) model (Sec. 3.4) and Artifact Classifier (Sec. 3.2). From this, we curate a high-quality subset of 20K (PRISM^LAYERS^{PRO}) and a broader 100K set (PRISM^LAYERS^{PLUS}) by automatic filtering. Additionally, we construct a 1K photorealistic dataset, PRISM^LAYERS^{REAL}. We then present dataset statistics and the curation pipeline, followed by our key technical contributions: LayerFLUX and MultiLayerFLUX (Sec. 3.3).154
155
3.1 PRISM^LAYERS STATISTICS
156157
158
159
160
161

Statistics on the number of layers. We analyze the distribution of transparent layer counts in PRISM^LAYERS and PRISM^LAYERS^{PRO}. For PRISM^LAYERS, each image contains an average of 7 layers (median: 6), with 79% of samples containing above 3 layers, while PRISM^LAYERS^{PRO} has an average of 9 layers (median: 9), with 90% of samples containing above 3 layers. This indicates that PRISM^LAYERS effectively captures a wide range of visual complexity. Figure 3 (a) provides a more detailed illustration of the transparent layer count distribution.

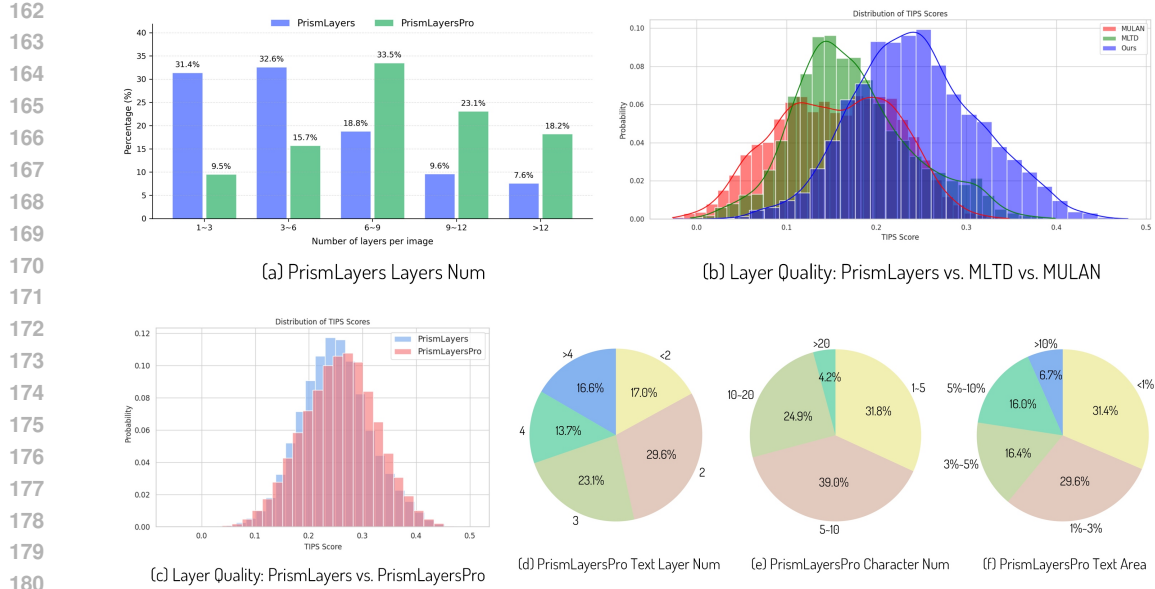


Figure 3: Illustrating the key dataset statistics on PRISM^LAYERS and PRISM^LAYERS^{PRO}. Subfigure (a) shows the layer number distribution for PRISM^LAYERS and PRISM^LAYERS^{PRO}. Subfigures (b) and (c) compare the Layer Quality (TIPS scores) of the PRISM^LAYERS dataset with the MLTD and MULAN datasets and PRISM^LAYERS with PRISM^LAYERS^{PRO}. Subfigures (d) through (f) detail the distribution of text layer count, character count, and text area within PRISM^LAYERS^{PRO}.

Statistics on the aesthetics of layers. A key contribution of this open-source dataset is the provision of aesthetically pleasing transparent layers, addressing the limited visual quality found in existing multi-layer datasets. As shown in Figure 3 (b), quantitative evaluations using our Transparent Image Aesthetic Scoring (TIPS) model illustrate the aesthetic distributions of PRISM^LAYERS, MULAN Tudosiu et al. (2024), and MLTD Pu et al. (2025). Figure 3 (c) further compares the aesthetic quality between PRISM^LAYERS and PRISM^LAYERS^{PRO}. PRISM^LAYERS^{PRO} increases the layers per image while achieving higher aesthetic quality compared to PRISM^LAYERS. Figure 4 visualizes qualitative comparisons between PRISM^LAYERS and PRISM^LAYERS^{PRO}. Our results show that PRISM^LAYERS consistently provides higher-quality layers, with the open-source subset PRISM^LAYERS^{PRO} achieving the best overall aesthetic quality.

Statistics of visual text layers. High-quality visual text rendering is essential for multi-layer transparent image generation, as textual elements play a central role in many business-centric visual designs Liu et al. (2024b;c). PRISM^LAYERS contains a large number of accurately rendered text layers, each isolated in a separate transparent channel. Figure 3 (d), (e), and (f) present statistics on the number of text layers per image, the number of characters per instance, and the area ratio of text layers.

Statistics of different visual styles. In the middle of Figure 1, we illustrate the distribution of transparent layers across different styles in PRISM^LAYERS^{PRO}, which contains 21 distinct styles. The top five most frequent styles are ‘toy’, ‘melting silver’, ‘line draw’, ‘ink’, and ‘doodle art’

Comparison with existing transparent datasets. Table 1 presents a comparison with previously existing multi-layer transparent image datasets. We position PRISM^LAYERS^{PRO} as the first open, high-quality synthetic dataset that supports a diverse range of layers, high-quality alpha mattes, and excellent aesthetic quality. We believe PRISM^LAYERS^{PRO} can serve as a solid foundation for future efforts in building better multi-layer transparent image generation models.

3.2 PRISM^LAYERS DATASET CURATION PROCESS

Multi-layer prompts and semantic layout from crawled data. **A** → **1** → **B** We begin by collecting an internal dataset of 800K multi-layer graphic designs sourced from various commercial websites. Each design instance consists of multiple transparent layers, including background elements,

Dataset	# Samples	# Layers	Open Source	Source Data	Alpha Quality	Aesthetic
Multi-layer Dataset Zhang & Agrawala (2024)	~ 1 M	2	✗	commercial, generated	good	good
LAION-L ² I Zhang et al. (2023)	~ 57 M	2	✗	LAION	normal	normal
MLCID Huang et al. (2024)	~ 2 M	[2,3,4]	✗	LAION	poor	poor
MLTD Pu et al. (2025)	~ 1 M	2 ~ 50	✗	Graphic design website	good	normal
MAGICK Burgert et al. (2024)	~ 150 K	1	✓	Synthetic	good	good
MuLAn Tudosiu et al. (2024)	~ 44 K	2 ~ 6	✓	COCO, LAION	poor	poor
Crello Yamaguchi (2021)	~ 20 K	2 ~ 50	✓	Graphic design website	normal	poor
PRISMLAYERS	~ 200 K	2 ~ 50	✓	Synthetic	good	good
PRISMLAYERSPLUS	~ 100 K	2 ~ 50	✓	Synthetic	good	good+
PRISMLAYERSPRO	~ 20 K	2 ~ 50	✓	Synthetic	good	excellent
PRISMLAYERSREAL	~ 1 K	1 ~ 8	✓	Synthetic	good	excellent

Table 1: Comparison with previous multi-layer transparent image datasets. This table presents a detailed comparison of publicly available and newly proposed multi-layer image datasets across several key dimensions, including the number of samples, the maximum number of layers, open-source status, source data origin, and two subjective quality metrics: Alpha Quality and Aesthetic appeal.



Figure 4: Illustrating the aesthetic quality of the crawled data (columns 1 and 4), synthetic data (columns 2 and 5), and high-quality synthetic data generated with a style prompt (columns 3 and 6).

decorations, text, and icons. To enrich the semantic understanding of each instance, we employ an off-the-shelf LLM—Llava 1.6 Liu et al. (2024a)—to generate captions for both individual transparent layers and the fully composed images. This process yields annotations comprising 800K multi-layer prompts and their corresponding semantic layouts, effectively capturing both the visual composition and the intended design semantics. We also extract the original metadata specifying the layer ordering for each graphic. For the filtered PRISMLAYERSPLUS and PRISMLAYERSPRO, we further enhance semantic richness by using GPT-4o to generate high-quality layer-wise captions.

Synthetic multi-layer transparent images with MultiLayerFLUX. **B** → **2** → **C** With the constructed 800K multi-layer prompts and corresponding semantic layout information, we apply a novel model, MultiLayerFLUX, to transform the layer-wise prompts into multiple transparent layers, each generated separately using a single-layer transparent image generation engine such as LayerFLUX, as illustrated in Sec. 3.3. We then composite these transparent layers onto a shared canvas, preserving the correct stacking order and ensuring seamless integration across layers. In total, creating the entire 800K multi-layer images takes around 7,000 A100 GPU hours.

Artifact multi-layer transparent image filter. **C** → **3** → **D** As MultiLayerFLUX generates each transparent layer separately and then combines them following the layer order, we observe severe artifacts in some synthetic multi-layer images. These artifacts include duplicate or similar layers positioned in conflicting spatial arrangements or exhibiting substantial and unreasonable overlap, as shown in Figure 6. To address this issue, we construct a reliable artifact classifier to further filter out flawed multi-layer transparent images. We begin by manually annotating severe artifacts in a subset of 8K synthetic multi-layer images with high aesthetic scores. Then, we train an artifact classifier by fine-tuning BLIP-2 Li et al. (2023) to predict confidence scores indicating whether a composed multi-layer transparent image contains such artifacts—e.g., conflicting layer placements or unreasonable overlap. To ensure the quality of the final dataset, we apply the trained classifier to select a subset of 200K synthetic multi-layer transparent images, forming PRISMLAYERS.

High-quality reference layout pool. **D** → **E** The aforementioned Artifact Classifier performs image-level structural assessment. Next, we perform visual quality filtering using an aesthetic predictor aes. We rank images with different numbers of layers based on their aesthetic scores, then select a fixed proportion of the highest-scoring images from each group to form an 80K-image high-quality reference layout pool.

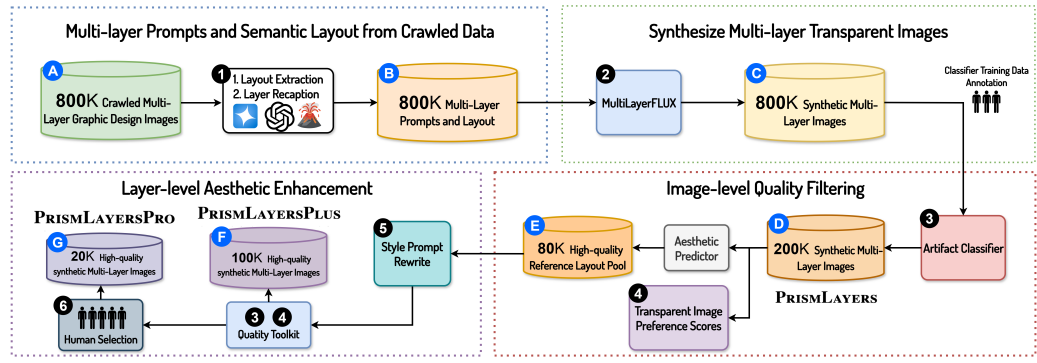


Figure 5: **Dataset Curation Pipeline of PRISM LAYERS, PRISM LAYERS PLUS, and PRISM LAYERS PRO.** We first extract semantic layouts from a database of 800K crawled multi-layer graphic design images. Then, we apply MultiLayerFLUX to generate high-quality multi-layer transparent images. An Artifact Classifier is used to evaluate the quality of each composed image, discarding low-quality results to construct PRISM LAYERS. We also apply the Transparent Image Preference Scores (TIPS) model to assess the quality of individual transparent layers. By filtering for aesthetic quality and balancing the number of layers, we collect an 80K-image reference layout pool. We sample layouts from this pool and regenerate them with style prompts, followed by quality evaluation and manual selection, forming our high-quality multi-layer dataset, PRISM LAYERS PLUS and PRISM LAYERS PRO.



Figure 6: Illustrating the artifact multi-layer transparent images that our classifier can identify and filter out.

295 Layer-wise quality filter, styled prompt rewrite, and human selection. $\textcolor{blue}{E} \rightarrow \textcolor{black}{\textcircled{5}} \rightarrow \textcolor{black}{\textcircled{3}} + \textcolor{black}{\textcircled{4}}$

296 $(+\textcolor{black}{\textcircled{6}}) \rightarrow \textcolor{black}{\textcircled{F}} (\textcolor{black}{\textcircled{G}})$ To improve layer quality, we construct two refined subsets from PRISM LAYERS: 297 20K PRISM LAYERS PRO and 100K PRISM LAYERS PLUS. The pipeline involves three steps: 1) Styled 298 prompt rewrite: we define 21 style keywords and sample layouts from the 80K reference pool. For 299 each style, 2K layouts (for PRISM LAYERS PRO) and 8K (for PRISM LAYERS PLUS) are selected. Their 300 layers are pasted onto a gray background and fed to GPT-4o, which rewrites captions with style 301 directives. MultiLayerFLUX then regenerates transparent layers from these captions. 2) Quality 302 Evaluation: we train the TIPS model on a collection of transparent images from our PRISM LAYERS, 303 single-layer images generated by LayerDiffuse Zhang & Agrawala (2024), and our reproduction 304 of LayerDiffuse based on FLUX.1-[dev]. The TIPS model is combined with Artifact Classifier to 305 evaluate both whole images and layers. 3) Human selection (for PRISM LAYERS PRO): top-quality 306 samples are manually selected by removing obvious failures with reference to the scores of quality 307 evaluation, while without the human selection, automatically filtered samples from PRISM LAYERS PLUS. 308 In practice, generating 20K PRISM LAYERS PRO with GPT refined annotations takes around 480 A100 309 GPU hours, while generating 100K PRISM LAYERS PLUS takes around 2,400 A100 GPU hours.

310 **Photorealistic multi-layer image synthesis.** Our approach primarily focuses on the design-oriented 311 synthesis of multi-layer datasets. Nevertheless, as shown in Figure 7, we also explore photorealistic 312 multi-layer image synthesis leveraging the prior knowledge from our collected multi-layer graphic 313 design images, resulting in a small but high-quality 1K dataset, PRISM LAYERS REAL, and we discuss 314 more details in Appendix N.



Figure 7: Illustrating the samples in PRISM LAYERS REAL.

322 **Discussion.** A natural question is whether the results exhibit cross-layer coherence. We acknowledge 323 this limitation, as synthetic multi-layer images cannot fully ensure consistency, though partial 324 mitigation is achieved via human selection. Importantly, we observe that training the recent ART



324
325
326
327
328
329
330
331
332
333
334
335
336
337
338
339
340
341
342
343
344
345
346
347
348
349
350
351
352
353
354
355
356
357
358
359
360
361
362
363
364
365
366
367
368
369
370
371
372
373
374
375
376
377
Figure 9: Attention maps between the *suffix text token* and *visual tokens*. We observe a clearly higher attention response in the background area with accurate boundary patterns.

model Pu et al. (2025) on our filtered high-quality dataset, yields noticeably improved coherence, underscoring the importance of high-quality supervision.

3.3 LAYERFLUX AND MULTILAYERFLUX

In this section, we present the mathematical formulation of the multi-layer transparent image generation task, followed by key insights and implementation details of our LayerFLUX and MultiLayerFLUX.

Formulation. The transparent image generation task aims to train a generative model that transform the input global text prompt $\mathbf{T}_{\text{global}}$ and the optional regional text prompts $\{\mathbf{T}_{\text{region}}^i\}_{i=1}^N$ into an output consisting of a set of transparent layers $\{\mathbf{I}_{\text{RGBA}}^i\}_{i=1}^N$ that can form a high-quality multi-layer image $\mathbf{I}_{\text{global}}$, and each layer is with accurate alpha channels $\{\mathbf{I}_{\text{alpha}}^i\}_{i=1}^N$. This task degrades to a single-layer transparent image generation task when $N = 1$. Following the latest ART Pu et al. (2025), we apply a flow matching model to model the multi-layer transparent image generation task by performing the latent denoising on the concatenation of both the global visual tokens and the regional visual tokens.

LayerFLUX. As shown in Figure 8, we build the LayerFLUX with two key designs, including the suffix prompt scheme and the additional salient object matting to predict the accurate alpha mattes.

Inspired by MAGICK Burgert et al. (2024), we design a series of tailored suffix prompts to guide diffusion models in generating images with single-colored, uniform backgrounds. These controlled conditions ensure that the foreground elements are clearly delineated, thereby simplifying the isolation process. Our implementation involves simply appending the suffix prompt “*isolated on a gray background*” to the original text prompt. Figure 9 visualizes the attention maps between the suffix tokens and the visual tokens. We also compare the results of using alternative suffix prompts by replacing the word “gray” with other colors. A detailed analysis of different suffix prompt effects is provided in Appendix L, M.

To extract accurate alpha mattes, we explore and evaluate multiple state-of-the-art image matting techniques, including SAM2 Ravi et al. (2024), BiRefNet Zheng et al. (2024), and RMBG-2.0 RMB, to separate the foreground from the background. This step is critical for producing high-quality, transparent images that can be seamlessly integrated into multi-layer compositions. We empirically find that RMBG-2.0 achieves the best matting quality, and we choose it as our default method.

MultiLayerFLUX. We construct the MultiLayerFLUX framework by stacking the outputs from the above-mentioned LayerFLUX according to the given layer-wise prompts and semantic layout. We observe that simply applying LayerFLUX to generate each layer within a fixed square canvas tends to produce objects with an unnatural square shape. Instead of generating each layer in a fixed square canvas, we preserve the original aspect ratio of each transparent layer and use FLUX.1-[dev] to generate images at varying resolutions, fixing the longer side to 1024. Each generated transparent layer is then resized to fit the corresponding bounding boxes based on the semantic layout information, and the layers are composited according to the layer-order annotations, resulting in the final synthetic multi-layer transparent images.

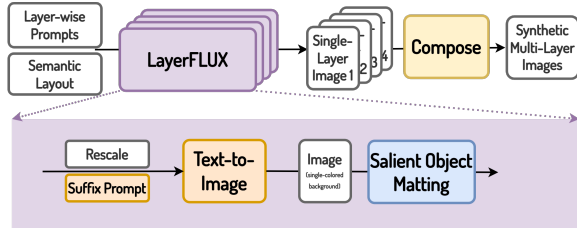


Figure 8: LayerFLUX and MultiLayerFLUX Framework.

378
379380 3.4 TRANSPARENT IMAGE QUALITY ASSESSMENT
381

382 Existing image quality assessment models Kirstain et al. (2024); Wu et al. (2023); Xu et al. (2024) are
383 primarily trained to predict human preferences for conventional RGB images, and thus are not well
384 suited for evaluating transparent images with alpha mattes. To address this gap, we propose a dedicated
385 quality scoring model tailored for transparent layer images. The core idea is to distill ensembled
386 preference signals—aggregated from multiple RGB-oriented models—into a model specialized for
387 transparent image quality, thereby mitigating model-specific biases.

388
389
390
391
392
393

394 **Transparent image preference dataset.** We first collect a transparent image preference (TIP) dataset
395 of more than 100K win-lose pairs by gathering three types of data resources, including those generated
396 with LayerFLUX and LayerDiffuse. We use multiple image quality scoring models to rate the quality
397 of each transparent layer, including Aesthetic Predictor V2.5 aes, Image Reward Xu et al. (2024),
398 LAION Aesthetic Predictor lai, HPSV2 Wu et al. (2023), and VQA Score Lin et al. (2024c). Then,
399 we compare each pair of transparent layers based on the weighted sum of the scores predicted by
400 the aforementioned quality scoring models. Here, we assume that the alpha mask quality of most
401 transparent layers generated with our LayerFLUX and LayerDiffuse methods is satisfactory.

402
403
404
405
406

407 **Transparent image preference score.** We train the transparent image preference scoring model by
408 fine-tuning CLIP on the TIP dataset. For each pair of transparent images with preference labels, we
409 choose loss function $\mathcal{L}_{\text{pref}} = (\log 1 - \log \mathbf{p}_w)$, where \mathbf{p}_w is the probability of the win image being
410 the preferred one, and we compute the \mathbf{p}_w as:

$$\mathbf{p}_w = \frac{\exp(\tau \cdot f_{\text{CLIP-V}}(\mathbf{I}^w) \cdot f_{\text{CLIP-T}}(\mathbf{T}))}{\exp(\tau \cdot f_{\text{CLIP-V}}(\mathbf{I}^w) \cdot f_{\text{CLIP-T}}(\mathbf{T})) + \exp(\tau \cdot f_{\text{CLIP-V}}(\mathbf{I}^l) \cdot f_{\text{CLIP-T}}(\mathbf{T}))}, \quad (1)$$

411
412
413
414
415

416 where $f_{\text{CLIP-V}}(\cdot)$ and $f_{\text{CLIP-T}}(\cdot)$ represent the CLIP visual encoder and text encoder separately. \mathbf{I}^w and
417 \mathbf{I}^l represent the preferred and dispreferred transparent image.

418
419
420
421
422
423
424
425
426
427
428
429
430
431

427 During the evaluation, we compute the transparent image preference score as follows:

$$\mathbf{p} = f_{\text{CLIP-V}}(\mathbf{I}) \cdot f_{\text{CLIP-T}}(\mathbf{T}), \quad (2)$$

428 where we directly use the dot product between the normalized CLIP visual embedding and the CLIP
429 text embedding as the transparent image preference score, abbreviated as TIPS for convenience.

430 4 EXPERIMENT

431
432
433
434
435
436
437
438
439
440
441
442
443
444
445
446
447
448
449
450
451
452
453
454
455
456
457
458
459
460
461
462
463
464
465
466
467
468
469
470
471
472
473
474
475
476
477
478
479
480
481
482
483
484
485
486
487
488
489
490
491
492
493
494
495
496
497
498
499
500
501
502
503
504
505
506
507
508
509
510
511
512
513
514
515
516
517
518
519
520
521
522
523
524
525
526
527
528
529
530
531
532
533
534
535
536
537
538
539
540
541
542
543
544
545
546
547
548
549
550
551
552
553
554
555
556
557
558
559
560
561
562
563
564
565
566
567
568
569
570
571
572
573
574
575
576
577
578
579
580
581
582
583
584
585
586
587
588
589
590
591
592
593
594
595
596
597
598
599
600
601
602
603
604
605
606
607
608
609
610
611
612
613
614
615
616
617
618
619
620
621
622
623
624
625
626
627
628
629
630
631
632
633
634
635
636
637
638
639
640
641
642
643
644
645
646
647
648
649
650
651
652
653
654
655
656
657
658
659
660
661
662
663
664
665
666
667
668
669
670
671
672
673
674
675
676
677
678
679
680
681
682
683
684
685
686
687
688
689
690
691
692
693
694
695
696
697
698
699
700
701
702
703
704
705
706
707
708
709
710
711
712
713
714
715
716
717
718
719
720
721
722
723
724
725
726
727
728
729
730
731
732
733
734
735
736
737
738
739
740
741
742
743
744
745
746
747
748
749
750
751
752
753
754
755
756
757
758
759
759
760
761
762
763
764
765
766
767
768
769
770
771
772
773
774
775
776
777
778
779
779
780
781
782
783
784
785
786
787
788
789
789
790
791
792
793
794
795
796
797
798
799
800
801
802
803
804
805
806
807
808
809
809
810
811
812
813
814
815
816
817
818
819
819
820
821
822
823
824
825
826
827
828
829
829
830
831
832
833
834
835
836
837
838
839
839
840
841
842
843
844
845
846
847
848
849
849
850
851
852
853
854
855
856
857
858
859
859
860
861
862
863
864
865
866
867
868
869
869
870
871
872
873
874
875
876
877
878
879
879
880
881
882
883
884
885
886
887
888
889
889
890
891
892
893
894
895
896
897
898
899
900
901
902
903
904
905
906
907
908
909
909
910
911
912
913
914
915
916
917
918
919
919
920
921
922
923
924
925
926
927
928
929
929
930
931
932
933
934
935
936
937
938
939
939
940
941
942
943
944
945
946
947
948
949
949
950
951
952
953
954
955
956
957
958
959
959
960
961
962
963
964
965
966
967
968
969
969
970
971
972
973
974
975
976
977
978
979
979
980
981
982
983
984
985
986
987
988
989
989
990
991
992
993
994
995
996
997
998
999
1000
1001
1002
1003
1004
1005
1006
1007
1008
1009
1009
1010
1011
1012
1013
1014
1015
1016
1017
1018
1019
1019
1020
1021
1022
1023
1024
1025
1026
1027
1028
1029
1029
1030
1031
1032
1033
1034
1035
1036
1037
1038
1039
1039
1040
1041
1042
1043
1044
1045
1046
1047
1048
1049
1049
1050
1051
1052
1053
1054
1055
1056
1057
1058
1059
1059
1060
1061
1062
1063
1064
1065
1066
1067
1068
1069
1069
1070
1071
1072
1073
1074
1075
1076
1077
1078
1079
1079
1080
1081
1082
1083
1084
1085
1086
1087
1088
1089
1089
1090
1091
1092
1093
1094
1095
1096
1097
1098
1099
1100
1101
1102
1103
1104
1105
1106
1107
1108
1109
1109
1110
1111
1112
1113
1114
1115
1116
1117
1118
1119
1119
1120
1121
1122
1123
1124
1125
1126
1127
1128
1129
1129
1130
1131
1132
1133
1134
1135
1136
1137
1138
1139
1139
1140
1141
1142
1143
1144
1145
1146
1147
1148
1149
1149
1150
1151
1152
1153
1154
1155
1156
1157
1158
1159
1159
1160
1161
1162
1163
1164
1165
1166
1167
1168
1169
1169
1170
1171
1172
1173
1174
1175
1176
1177
1178
1179
1179
1180
1181
1182
1183
1184
1185
1186
1187
1188
1189
1189
1190
1191
1192
1193
1194
1195
1196
1197
1198
1199
1199
1200
1201
1202
1203
1204
1205
1206
1207
1208
1209
1209
1210
1211
1212
1213
1214
1215
1216
1217
1218
1219
1219
1220
1221
1222
1223
1224
1225
1226
1227
1228
1229
1229
1230
1231
1232
1233
1234
1235
1236
1237
1238
1239
1239
1240
1241
1242
1243
1244
1245
1246
1247
1248
1249
1249
1250
1251
1252
1253
1254
1255
1256
1257
1258
1259
1259
1260
1261
1262
1263
1264
1265
1266
1267
1268
1269
1269
1270
1271
1272
1273
1274
1275
1276
1277
1278
1279
1279
1280
1281
1282
1283
1284
1285
1286
1287
1288
1289
1289
1290
1291
1292
1293
1294
1295
1296
1297
1298
1299
1299
1300
1301
1302
1303
1304
1305
1306
1307
1308
1309
1309
1310
1311
1312
1313
1314
1315
1316
1317
1318
1319
1319
1320
1321
1322
1323
1324
1325
1326
1327
1328
1329
1329
1330
1331
1332
1333
1334
1335
1336
1337
1338
1339
1339
1340
1341
1342
1343
1344
1345
1346
1347
1348
1349
1349
1350
1351
1352
1353
1354
1355
1356
1357
1358
1359
1359
1360
1361
1362
1363
1364
1365
1366
1367
1368
1369
1369
1370
1371
1372
1373
1374
1375
1376
1377
1378
1379
1379
1380
1381
1382
1383
1384
1385
1386
1387
1388
1389
1389
1390
1391
1392
1393
1394
1395
1396
1397
1398
1399
1399
1400
1401
1402
1403
1404
1405
1406
1407
1408
1409
1409
1410
1411
1412
1413
1414
1415
1416
1417
1418
1419
1420
1421
1422
1423
1424
1425
1426
1427
1428
1429
1430
1431
1432
1433
1434
1435
1436
1437
1438
1439
1439
1440
1441
1442
1443
1444
1445
1446
1447
1448
1449
1449
1450
1451
1452
1453
1454
1455
1456
1457
1458
1459
1459
1460
1461
1462
1463
1464
1465
1466
1467
1468
1469
1469
1470
1471
1472
1473
1474
1475
1476
1477
1478
1479
1479
1480
1481
1482
1483
1484
1485
1486
1487
1488
1489
1489
1490
1491
1492
1493
1494
1495
1496
1497
1498
1499
1499
1500
1501
1502
1503
1504
1505
1506
1507
1508
1509
1509
1510
1511
1512
1513
1514
1515
1516
1517
1518
1519
1519
1520
1521
1522
1523
1524
1525
1526
1527
1528
1529
1529
1530
1531
1532
1533
1534
1535
1536
1537
1538
1539
1539
1540
1541
1542
1543
1544
1545
1546
1547
1548
1549
1549
1550
1551
1552
1553
1554
1555
1556
1557
1558
1559
1559
1560
1561
1562
1563
1564
1565
1566
1567
1568
1569
1569
1570
1571
1572
1573
1574
1575
1576
1577
1578
1579
1579
1580
1581
1582
1583
1584
1585
1586
1587
1588
1589
1589
1590
1591
1592
1593
1594
1595
1596
1597
1598
1599
1599
1600
1601
1602
1603
1604
1605
1606
1607
1608
1609
1609
1610
1611
1612
1613
1614
1615
1616
1617
1618
1619
1619
1620
1621
1622
1623
1624
1625
1626
1627
1628
1629
1629
1630
1631
1632
1633
1634
1635
1636
1637
1638
1639
1639
1640
1641
1642
1643
1644
1645
1646
1647
1648
1649
1649
1650
1651
1652
1653
1654
1655
1656
1657
1658
1659
1659
1660
1661
1662
1663
1664
1665
1666
1667
1668
1669
1669
1670
1671
1672
1673
1674
1675
1676
1677
1678
1679
1679
1680
1681
1682
1683
1684
1685
1686
1687
1688
1689
1689
1690
1691
1692
1693
1694
1695
1696
1697
1698
1699
1699
1700
1701
1702
1703
1704
1705
1706
1707
1708
1709
1709
1710
1711
1712
1713
1714
1715
1716
1717
1718
1719
1719
1720
1721
1722
1723
1724
1725
1726
1727
1728
1729
1729
1730
1731
1732
1733
1734
1735
1736
1737
1738
1739
1739
1740
1741
1742
1743
1744
1745
1746
1747
1748
1749
1749
1750
1751
1752
1753
1754
1755
1756
1757
1758
1759
1759
1760
1761
1762
1763
1764
1765
1766
1767
1768
1769
1769
1770
1771
1772
1773
1774
1775
1776
1777
1778
1779
1779
1780
1781
1782
1783
1784
1785
1786
1787
1788
1789
1789
1790
1791
1792
1793
1794
1795
1796
1797
1798
1799
1799
1800
1801
1802
1803
1804
1805
1806
1807
1808
1809
1809
1810
1811
1812
1813
1814
1815
1816
1817
1818
1819
1819
1820
1821
1822
1823
1824
1825
1826
1827
1828
1829
1829
1830
1831
1832
1833
1834
1835
1836
1837
1838
1839
1839
1840
1841
1842
1843
1844
1845
1846
1847
1848
1849
1849
1850
1851
1852
1853
1854
1855
1856
1857
1858
1859
1859
1860
1861
1862
1863
1864
1865
1866
1867
1868
1869
1869
1870
1871
1872
1873
1874
1875
1876
1877
1878
1879
1879
1880
1881
1882
1883
1884
1885
1886
1887
1888
1889
1889
1890
1891
1892
1893
1894
1895
1896
1897
1898
1899
1899
1900
1901
1902
1903
1904
1905
1906
1907
1908
1909
1909
1910
1911
1912
1913
1914
1915
1916
1917
1918
1919
1919
1920
1921
1922
1923
1924
1925
1926
1927
1928
1929
1929
1930
1931
1932
1933
1934
1935
1936
1937
1938
1939
1939
1940
1941
1942
1943
1944
1945
1946
1947
1948
1949
1949
1950
1951
1952
1953
1954
1955
1956
1957
1958
1959
1959
1960
1961
1962
1963
1964
1965
1966
1967
1968
1969
1969
1970
1971
1972
1973
1974
1975
1976
1977
1978
1979
1979
1980
1981
1982
1983
1984
1985
1986
1987
1988
1989
1989
1990
1991
1992
1993
1994
1995
1996
1997
1998
1999
1999
2000
2001
2002
2003
2004
2005
2006
2007
2008
2009
2010
2011
2012
2013
2014
2015
2016
2017
2018
2019
2020
2021
2022
2023
2024
2025
2026
2027
2028
2029
2030
2031
2032
2033
2034
2035
2036
2037
2038
2039
2040
2041
2042
2043
2044
2045
2046
2047
2048
2049



Figure 10: Qualitative comparison results between ART (top row) and ART+ (bottom row).

Method	DESIGN-MULTI-LAYER-BENCH				FLUX-MULTI-LAYER-BENCH			
	FID _{merged} ↓	TIPS	PSNR	SSIM	FID _{merged} ↓	TIPS	PSNR	SSIM
ART Pu et al. (2025)	<u>18.34</u>	16.84	27.41	0.9490	30.04	16.64	26.99	0.9502
MultiLayerFLUX	21.29	<u>19.90</u>	-	-	29.64	<u>20.65</u>	-	-
ART+(20k scratch)	26.53	18.91	<u>28.12</u>	<u>0.9544</u>	26.07	19.42	<u>28.12</u>	0.9559
ART+(20k)	21.66	18.82	27.90	0.9536	<u>25.23</u>	18.98	28.06	<u>0.9560</u>
ART+(100k)	25.11	18.13	26.71	0.9423	25.63	18.27	26.80	0.9455

Table 3: Quantitative comparison of our ART+ with the state-of-the-art ART and our proposed MultiLayerFLUX. The best metric value in each column is indicated with an underline.

User Study Evaluation. To assess the effectiveness of our dataset and fine-tuning strategy, we conduct a user study comparing ART+(20k scratch) with the original ART, PRISM^LAYERS, and PRISM^LAYERS^{PRO}. The study involves 40 representative samples from FLUX-MULTI-LAYER-BENCH, with over 20 participants evaluating three key dimensions: (i) *Layer Quality* (visual aesthetics and alpha fidelity), (ii) *Global Harmonization* (inter-layer coherence), and (iii) *Prompt Following* (alignment with input prompts).

As shown in Figure 2, ART+(20k scratch) outperforms the original ART with average win rates of 57.9% in layer quality and 59.3% in prompt following. It also surpasses MultiLayerFLUX in global harmonization (45.1% win rate), validating the impact of combining high-quality supervision with task-specific tuning.

Quantitative Results. Table 3 presents a comprehensive comparison between our ART+ model and the current state-of-the-art (SOTA) model on two benchmarks with different data distributions. For ART+, the MLTD (800K) and PrismLayers (200K) datasets are used for fine-tuning the base FLUX model (similar to the ART approach), while PrismLayersPro and PrismLayersPlus are used for subsequent high-quality fine-tuning following Dai et al. (2023). We evaluated four key metrics: FID_{merged} and TIPS for image and layer quality, and PSNR and SSIM for transparent decoding quality. The results consistently demonstrate that our ART+ model achieves superior performance across these metrics, establishing it as the new SOTA.

For the FID_{merged} score, our ART+ significantly outperforms ART on FLUX-MULTI-LAYER-BENCH. We also provide additional qualitative comparison results to support this finding. An interesting phenomenon, however, is that ART demonstrates superior performance on DESIGN-MULTI-LAYER-BENCH. This can be attributed to the significant similarity between ART’s training data distribution and this benchmark, a more detailed analysis of which is provided in Appendix.D.

Regarding the TIPS scores, we note a partial data overlap between the training data of ART+(20k scratch) and the TIPS evaluation set. While this might be a concern for fairness, our more extensive testing of ART+(20k) and ART+(100k) — where this overlap does not exist — effectively mitigates this issue. All results consistently show that the layer quality of ART+ is far superior to ART and approaches that of the original FLUX.

Across all metrics, the performance of ART+(100k) is comparable to ART+(20k) and surpasses ART. This demonstrates that our automated approach can efficiently build high-quality, reproducible training data on a large scale without the need for human intervention.

Qualitative MultiLayer Results. Figure 11 presents qualitative results comparing our MultiLayerFLUX with the fine-tuned ART+, while Figure 10 shows qualitative comparisons between ART and the fine-tuned ART+. We observe that ART+ achieves significantly better global harmonization than



Figure 11: Qualitative comparison results between MultiLayerFLUX (top row) and ART+ (bottom row).



Figure 12: Qualitative comparison results between FLUX.1-[dev] (1st row), MultiLayerFLUX (2nd row), ART (3rd row), and ART+ (4th row) across 7 cases (columns). The rightmost columns show composed multi-layer images.

MultiLayerFLUX and better layer quality than ART, separately. These comparisons reveal that the fine-tuned ART+ achieves an excellent balance between layer quality and global harmonization.

Comparison to FLUX. Figure 12 compares the merged multi-layer image generation results with the reference ideal images generated directly with FLUX.1-[dev]. We can see that our ART+ significantly outperforms ART and MultiLayerFLUX, achieving aesthetics very close to those of the original modern text-to-image generation models.

5 CONCLUSION

This paper has tackled the significant gap in multi-layer transparent image generation by assembling and releasing four open, ultra-high-fidelity datasets—PRISM^LAYERS (200K samples), PRISM^LAYERS^PLUS (100K samples), PRISM^LAYERS^PRO (20K samples), and PRISM^LAYERS^REAL (1K samples)—each annotated with precise alpha mattes. To produce this data on demand, we devised a training-free synthesis pipeline that harnesses off-the-shelf diffusion models, and we built two complementary methods: LayerFLUX and MultiLayerFLUX. After rigorous artifact filtering and human validation, we fine-tuned the ART model on PRISM^LAYERS^PRO to obtain ART+, which outperforms the original ART in 60% of head-to-head user studies and matches the visual quality of top text-to-image models. By establishing this open dataset, synthesis pipeline, and strong baseline, we lay a solid foundation for future research and applications in precise, editable, and visually compelling multi-layer transparent image generation.

540
541 ETHICS STATEMENT542
543 Our work does not appear to raise major ethical concerns. The dataset used in this work is entirely
544 synthetic, generated without involving real human subjects. During the data generation process, we
545 applied filtering mechanisms to exclude outputs that may pose potential ethical concerns.
546546
547 REPRODUCIBILITY STATEMENT548
549 All experiments and synthetic data generation were conducted on NVIDIA A100 GPUs. To facilitate
550 reproducibility, we provide a detailed description of the pipeline and algorithms used to construct
551 the dataset, which are straightforward and reproducible. We also illustrate all experimental settings,
552 training details, and evaluation protocols within the paper and appendix. In addition, we will release
553 the dataset in the future to ensure reproduction and enable further research.
554

555 REFERENCES

556 Rmbg-2.0. <https://huggingface.co/briaai/RMBG-2.0>.
557 Aesthetic score v2.5. <https://github.com/discus0434/aesthetic-predictor-v2-5>.
558 Flux. <https://github.com/black-forest-labs/flux/>.
559 Laion aesthetic. <https://github.com/LAION-AI/aesthetic-predictor>.
560 Shuai Bai, Yuxuan Cai, Ruizhe Chen, Keqin Chen, Xionghui Chen, Zesen Cheng, Lianghao Deng, Wei
561 Ding, Chang Gao, Chunjiang Ge, et al. Qwen3-vl technical report. *arXiv preprint arXiv:2511.21631*,
562 2025.
563 Ryan D Burgert, Brian L Price, Jason Kuen, Yijun Li, and Michael S Ryoo. Magick: A large-scale
564 captioned dataset from matting generated images using chroma keying. In *CVPR*, pp. 22595–22604,
565 2024.
566 Nicolas Carion, Laura Gustafson, Yuan-Ting Hu, Shoubhik Debnath, Ronghang Hu, Didac Suris,
567 Chaitanya Ryali, Kalyan Vasudev Alwala, Haitham Khedr, Andrew Huang, et al. Sam 3: Segment
568 anything with concepts. *arXiv preprint arXiv:2511.16719*, 2025.
569 Yutao Cheng, Zhao Zhang, Maoke Yang, Hui Nie, Chunyuan Li, Xinglong Wu, and Jie Shao. Graphic
570 design with large multimodal model. *arXiv preprint arXiv:2404.14368*, 2024.
571 Xiaoliang Dai, Ji Hou, Chih-Yao Ma, Sam Tsai, Jialiang Wang, Rui Wang, Peizhao Zhang, Simon
572 Vandenhende, Xiaofang Wang, Abhimanyu Dubey, et al. Emu: Enhancing image generation
573 models using photogenic needles in a haystack. *arXiv preprint arXiv:2309.15807*, 2023.
574 Dingbang Huang, Wenbo Li, Yifei Zhao, Xinyu Pan, Yanhong Zeng, and Bo Dai. PSDiffusion:
575 Harmonized Multi-Layer Image Generation via Layout and Appearance Alignment, May 2025a.
576 URL <http://arxiv.org/abs/2505.11468>. arXiv:2505.11468 [cs].
577 Junjia Huang, Pengxiang Yan, Jinhang Cai, Jiyang Liu, Zhao Wang, Yitong Wang, Xinglong Wu,
578 and Guanbin Li. DreamLayer: Simultaneous Multi-Layer Generation via Diffusion Mode, March
579 2025b. URL <http://arxiv.org/abs/2503.12838>. arXiv:2503.12838 [cs].
580 Runhui Huang, Kaixin Cai, Jianhua Han, Xiaodan Liang, Renjing Pei, Guansong Lu, Songcen Xu,
581 Wei Zhang, and Hang Xu. LayerDiff: Exploring text-guided multi-layered composable image
582 synthesis via layer-collaborative diffusion model. In *ECCV*, 2024.
583 Naoto Inoue, Kento Masui, Wataru Shimoda, and Kota Yamaguchi. Opencole: Towards reproducible
584 automatic graphic design generation. In *CVPR*, pp. 8131–8135, 2024.
585 Peidong Jia, Chenxuan Li, Yuhui Yuan, Zeyu Liu, Yichao Shen, Bohan Chen, Xingru Chen, Yinglin
586 Zheng, Dong Chen, Ji Li, et al. Cole: A hierarchical generation framework for multi-layered and
587 editable graphic design. *arXiv preprint arXiv:2311.16974*, 2023.

594 Kyoungkook Kang, Gyujin Sim, Geonung Kim, Donguk Kim, Seungho Nam, and Sunghyun Cho.
 595 Layeringdiff: Layered image synthesis via generation, then disassembly with generative knowledge.
 596 *arXiv preprint arXiv:2501.01197*, 2025.

597

598 Kotaro Kikuchi, Naoto Inoue, Mayu Otani, Edgar Simo-Serra, and Kota Yamaguchi. Multimodal
 599 markup document models for graphic design completion. *arXiv preprint arXiv:2409.19051*, 2024.

600 Yuval Kirstain, Adam Polyak, Uriel Singer, Shahbuland Matiana, Joe Penna, and Omer Levy.
 601 Pick-a-pic: An open dataset of user preferences for text-to-image generation. *NeurIPS*, 36, 2024.

602

603 Junnan Li, Dongxu Li, Silvio Savarese, and Steven Hoi. Blip-2: Bootstrapping language-image
 604 pre-training with frozen image encoders and large language models. In *International conference
 605 on machine learning*, pp. 19730–19742. PMLR, 2023.

606 Jiawei Lin, Shizhao Sun, Danqing Huang, Ting Liu, Ji Li, and Jiang Bian. From elements to design:
 607 A layered approach for automatic graphic design composition. *arXiv preprint arXiv:2412.19712*,
 608 2024a.

609

610 Jieru Lin, Danqing Huang, Tiejun Zhao, Dechen Zhan, and Chin-Yew Lin. Designprobe: A graphic
 611 design benchmark for multimodal large language models. *arXiv preprint arXiv:2404.14801*, 2024b.

612 Kevin Lin, Zhengyuan Yang, Linjie Li, Jianfeng Wang, and Lijuan Wang. Designbench: Exploring
 613 and benchmarking dall-e 3 for imagining visual design. *arXiv preprint arXiv:2310.15144*, 2023.

614 Zhiqiu Lin, Deepak Pathak, Baiqi Li, Jiayao Li, Xide Xia, Graham Neubig, Pengchuan Zhang, and
 615 Deva Ramanan. Evaluating text-to-visual generation with image-to-text generation. In *ECCV*, pp.
 616 366–384. Springer, 2024c.

617

618 Haotian Liu, Chunyuan Li, Yuheng Li, Bo Li, Yuanhan Zhang, Sheng Shen, and Yong Jae Lee.
 619 Llava-next: Improved reasoning, ocr, and world knowledge, January 2024a. URL <https://llava-vl.github.io/blog/2024-01-30-llava-next/>.

620

621 Zeyu Liu, Weicong Liang, Zhanhao Liang, Chong Luo, Ji Li, Gao Huang, and Yuhui Yuan. Glyph-byt5:
 622 A customized text encoder for accurate visual text rendering. In *European Conference on Computer
 623 Vision*, pp. 361–377. Springer, 2024b.

624

625 Zeyu Liu, Weicong Liang, Yiming Zhao, Bohan Chen, Lin Liang, Lijuan Wang, Ji Li, and Yuhui
 626 Yuan. Glyph-byt5-v2: A strong aesthetic baseline for accurate multilingual visual text rendering.
 627 *arXiv preprint arXiv:2406.10208*, 2024c.

628

629 Yuyang Peng, Shishi Xiao, Keming Wu, Qisheng Liao, Bohan Chen, Kevin Lin, Danqing Huang,
 630 Ji Li, and Yuhui Yuan. Bizgen: Advancing article-level visual text rendering for infographics
 631 generation. *arXiv preprint arXiv:2503.20672*, 2025.

632

633 Dustin Podell, Zion English, Kyle Lacey, Andreas Blattmann, Tim Dockhorn, Jonas Müller, Joe
 634 Penna, and Robin Rombach. Sdxl: Improving latent diffusion models for high-resolution image
 635 synthesis. *arXiv preprint arXiv:2307.01952*, 2023.

636

637 Yifan Pu, Yiming Zhao, Zhicong Tang, Ruihong Yin, Haoxing Ye, Yuhui Yuan, Dong Chen, Jianmin
 638 Bao, Sirui Zhang, Yanbin Wang, Lin Liang, Lijuan Wang, Ji Li, Xiu Li, Zhouhui Lian, Gao Huang,
 639 and Baining Guo. Art: Anonymous region transformer for variable multi-layer transparent image
 640 generation. In *CVPR*, 2025.

641

642 Nikhila Ravi, Valentin Gabeur, Yuan-Ting Hu, Ronghang Hu, Chaitanya Ryali, Tengyu Ma, Haitham
 643 Khedr, Roman Rädle, Chloe Rolland, Laura Gustafson, et al. Sam 2: Segment anything in images
 644 and videos. *arXiv preprint arXiv:2408.00714*, 2024.

645

646 Mohammad Amin Shabani, Zhaowen Wang, Difan Liu, Nanxuan Zhao, Jimei Yang, and Yasutaka
 647 Furukawa. Visual layout composer: Image-vector dual diffusion model for design layout generation.
 648 In *CVPR*, pp. 9222–9231, 2024.

649

650 Petru-Daniel Tudosiu, Yongxin Yang, Shifeng Zhang, Fei Chen, Steven McDonagh, Gerasimos
 651 Lampouras, Ignacio Iacobacci, and Sarah Parisot. Mulan: A multi layer annotated dataset for
 652 controllable text-to-image generation. In *CVPR*, pp. 22413–22422, 2024.

648 Haohan Weng, Danqing Huang, Yu Qiao, Zheng Hu, Chin-Yew Lin, Tong Zhang, and CL Chen.
649 Design: A pipeline for controllable design template generation. In *CVPR*, pp. 12721–12732, 2024.
650

651 Chenfei Wu, Jiahao Li, Jingren Zhou, Junyang Lin, Kaiyuan Gao, Kun Yan, Sheng-ming Yin, Shuai
652 Bai, Xiao Xu, Yilei Chen, et al. Qwen-image technical report. *arXiv preprint arXiv:2508.02324*,
653 2025.

654 Xiaoshi Wu, Yiming Hao, Keqiang Sun, Yixiong Chen, Feng Zhu, Rui Zhao, and Hongsheng Li.
655 Human preference score v2: A solid benchmark for evaluating human preferences of text-to-image
656 synthesis. *arXiv preprint arXiv:2306.09341*, 2023.

657 Jiazheng Xu, Xiao Liu, Yuchen Wu, Yuxuan Tong, Qinkai Li, Ming Ding, Jie Tang, and Yuxiao Dong.
658 Imagereward: Learning and evaluating human preferences for text-to-image generation. *NeurIPS*,
659 36, 2024.

660 Kota Yamaguchi. Canvasvae: Learning to generate vector graphic documents. In *Proceedings of the
661 IEEE/CVF International Conference on Computer Vision*, pp. 5481–5489, 2021.

662 Lvmin Zhang and Maneesh Agrawala. Transparent image layer diffusion using latent transparency.
663 *arXiv preprint arXiv:2402.17113*, 2024.

664 Xinyang Zhang, Wentian Zhao, Xin Lu, and Jeff Chien. Text2Layer: Layered image generation using
665 latent diffusion model. *arXiv:2307.09781*, 2023.

666 Peng Zheng, Dehong Gao, Deng-Ping Fan, Li Liu, Jorma Laaksonen, Wanli Ouyang, and Nicu
667 Sebe. Bilateral reference for high-resolution dichotomous image segmentation. *CAAI Artificial
668 Intelligence Research*, 3:9150038, 2024.

669

670

671

672

673

674

675

676

677

678

679

680

681

682

683

684

685

686

687

688

689

690

691

692

693

694

695

696

697

698

699

700

701

702 **LLM usage.** We use Large Language Models (LLMs) to assist in synthetic image annotation and
 703 text-to-image (T2I) prompt generation.
 704

705 **A. Details of Suffix Prompt Templates** Table 4 illustrates the detailed suffix prompt templates we
 706 adopted for LayerFLUX.

Method	detailed prompt
709 SuffixPrompt A	on a solid plain gray background.
710 SuffixPrompt B	with a clear, solid gray background.
711 SuffixPrompt C	on a solid single gray background.
712 SuffixPrompt D	floating with a background that is solid gray.
713 SuffixPrompt E	cut-out on a solid gray background.
714 SuffixPrompt F	standing on a background that is fully solid gray
715 SuffixPrompt G	without any surrounding details
716 SuffixPrompt H	isolated on a solid gray background

717 Table 4: Effect of choosing different suffix prompt templates.
 718

719 **B. Generating Multi-Page and Multi-Layer Transparent Slides.** We plan to extend our approach
 720 to generate multi-page, multi-layer transparent slides. Our framework not only produces single-layer
 721 transparent images but also assembles them into coherent slide decks with multiple pages. Each
 722 slide is constructed from several transparent layers, with each layer corresponding to different design
 723 elements. This modular, bottom-up strategy enables precise control over both the spatial layout and
 724 stylistic attributes of each slide, ensuring consistency across pages while preserving the flexibility to
 725 customize individual layers.

726 **C.Explanation of the Benchmarks** Here, we provide a detailed explanation of the composition of
 727 our two benchmarks: DESIGN-MULTI-LAYER-BENCH and FLUX-MULTI-LAYER-BENCH.
 728

729 DESIGN-MULTI-LAYER-BENCH is a validation set originally introduced in the ART Pu et al. (2025).
 730 This dataset comprises 5,000 samples constructed from templates on popular graphic design platforms
 731 such as VistaCreate and Canva. A key characteristic of this benchmark is that its ground-truth
 732 reference images were manually created by human designers, though their style is primarily restricted
 733 to flat design. The data distribution of this benchmark is nearly identical to that of the ART training
 734 data.

735 In contrast, FLUX-MULTI-LAYER-BENCH is our newly developed validation set, also containing 5,000
 736 samples. The core difference lies in its ground-truth reference images, which are high-quality, single-
 737 layer images generated by the FLUX-1-[dev] model. This benchmark is specifically designed to more
 738 accurately measure the visual fidelity gap between generated multi-layer images and state-of-the-art
 739 text-to-image models. Furthermore, this dataset encompasses a more diverse range of graphic design
 740 styles, thereby addressing the stylistic uniformity limitation of the former benchmark.

741 **D. Discussion about FID on the DESIGN-MULTI-LAYER-BENCH** Despite the significant improvements
 742 made by the ART+ model, its FID (Fréchet Inception Distance) score on the DESIGN-MULTI-LAYER-
 743 BENCH is unexpectedly higher than that of the original ART model. This counterintuitive result is
 744 primarily due to two core reasons:

745 First, the FID metric measures the statistical distance between feature distributions in the Inception-v3
 746 feature space. The ground-truth reference images in the DESIGN-MULTI-LAYER-BENCH are heavily
 747 concentrated on a specific flat graphic design style. In contrast, our ART+ model was fine-tuned
 748 on the PrismLayers/PrismLayersPro dataset, which is designed to generate more diverse, higher-
 749 quality transparent layers across a broader range of styles. Consequently, the feature distribution
 750 of the ART+ model’s outputs diverges significantly from the narrow, flat-design distribution of the
 751 DESIGN-MULTI-LAYER-BENCH, leading to the FID metric unfairly penalizing the model’s increased
 752 diversity.

753 To more reliably assess the visual quality of the generated transparent layers, we constructed the
 754 FLUX-MULTI-LAYER-BENCH, whose ground-truth reference images are high-quality outputs from the
 755 state-of-the-art text-to-image model FLUX-1-[dev]. On this benchmark, our ART+ model achieves a
 lower FID score, which strongly validates the benefits of our training with PrismLayers. Additionally,

756 we also demonstrate that ART+ can generate multi-layer images with much better aesthetics, as shown
 757 in Figure 10 and 12.

759 In conclusion, FID primarily measures the closeness of two feature distributions, not necessarily
 760 the perceptual quality of the images themselves. Therefore, a fair comparison requires a test set
 761 that aligns with the model’s target data distribution. The suboptimal performance of ART+ on the
 762 DESIGN-MULTI-LAYER-BENCH is a direct consequence of a data distribution mismatch. For future
 763 work, we welcome and encourage further exploration into developing a more suitable evaluation
 764 metric than FID.

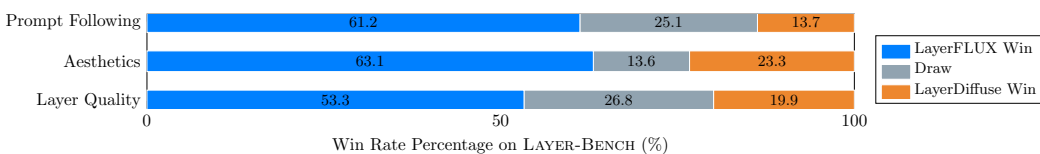
765 **E. Side Effect of Suffix Prompt.** We admit that adding the suffix prompt is not a free lunch and
 766 report the results of adding the suffix prompt on the GenEval benchmark in Table 5. We can see that
 767 the prompt-following capability of the original text-to-image generation model slightly drops, while
 768 the visual aesthetics are maintained.

Model	Overall	Single	Two	Counting	Colors	Position	Color
FLUX.1-[dev]	0.657	0.978	0.816	0.716	0.801	0.228	0.405
FLUX.1-[dev] + suffix prompt	0.591	0.906	0.609	0.628	0.723	0.313	0.370

773 Table 5: Comparison results on GenEval.

775 **F. Technical Details of LayerDiffuse with FLUX.** Our implementation of Layerdiffuse with FLUX
 776 is built on FLUX.1-[Dev] with LoRA. Specifically, we convert the image in the MAGICK dataset to
 777 grayscale according to the alpha channel mask. After training, the model is capable of generating
 778 grayscale background images without the need for additional conditional inputs. Then, we train a
 779 transparency VAE decoder to enable the prediction of alpha channels. The decoder is trained on both
 780 the MAGICK dataset and an internal dataset, thereby enhancing its robustness and generalization.
 781 For the text sticker, we collect a 5k dataset and use GPT-4o to reception of the image.

782 **G. Experiment Results of LayerFLUX.** We construct a LAYER-BENCH to evaluate the quality of the
 783 single-layer transparent images generated by our LayerFLUX. The LAYER-BENCH consists of 1,500
 784 prompts divided into three types of prompt sets: (i) one that primarily focuses on natural objects
 785 sampled from the MAGICK Burgert et al. (2024) set, where each prompt describes a photorealistic
 786 object; (ii) one centers on stickers and text stickers, where the text stickers contains visual text designed
 787 in creative typography and style to make the words stand out as part of the visual design; and (iii)
 788 one is about creative and stylistic objects. We construct the test set of stickers and text stickers by
 789 recaptioning sticker images crawled from the internet.



796 Figure 13: Illustrating the win-rate on single-layer transparent image generation benchmark LAYER-BENCH.



807 Figure 14: Qualitative comparison of results with SOTA on LAYER-BENCH. The first row shows the results
 808 generated with LayerDiffuse, while the second row shows the results generated with our LayerFLUX.

809 We compare our approach to the latest state-of-the-art transparent image generation LayerDiffuse Zhang
 & Agrawala (2024) by involving more than ~ 20 participants from diverse backgrounds in AI, graphic

# samples	TIPS (Layer Quality)	Composed Image Quality
Baseline (ART)	0.114 \pm 0.077	4.674 \pm 0.373
10	0.110 \pm 0.076	4.684 \pm 0.543
100	0.130 \pm 0.086	4.938 \pm 0.418
1000	0.135 \pm 0.080	4.936 \pm 0.415

Table 6: Effect of the high-quality data scale.

Method	Natural Object Layer Quality			Sticker Layer Quality			Creative Object Layer Quality		
	HPSv2 \uparrow	AE-V2.5 \uparrow	TIPS \uparrow	HPSv2 \uparrow	AE-V2.5 \uparrow	TIPS \uparrow	HPSv2 \uparrow	AE-V2.5 \uparrow	TIPS \uparrow
LayerDiffuse Zhang & Agrawala (2024)	26.28	5.451	29.37	21.51	3.640	19.11	29.13	5.057	32.53
LayerDiffuse w/ FLUX	24.33	5.374	27.65	25.79	4.376	25.16	25.25	4.974	29.09
Ours	26.58	5.617	30.19	26.14	4.735	25.69	29.55	5.551	36.25

Table 7: Comparison with LayerDiffuse on LAYER-BENCH.

design, art, and marketing. We present system level comparison in Table 7 and the user study results and visual comparisons in Figure 13 and Figure 14. We can see that our LayerFLUX achieves better results across the three types of prompt sets, especially in the creative, stylistic, or text sticker prompt sets. For example, our LayerFLUX achieves better layer quality and prompt following than LayerDiffuse, with win-rates of 63.1% and 61.2% when evaluated on our LAYER-BENCH. One possible concern might be that LayerDiffuse is built on SDXL Podell et al. (2023) rather than FLUX.1-[dev]. We also fine-tune LayerDiffuse on existing transparent image datasets based on FLUX, but we find that the performance is even worse than that of the original LayerDiffuse based on SDXL. We infer that *a key reason is that the quality of data generated by these powerful models (like FLUX.1-[dev]) significantly outperforms that of existing transparent images available on the internet or predicted by existing models*. This widening quality gap makes it risky to fine-tune them directly. In summary, our training-free LayerFLUX can better maintain the original capabilities of the off-the-shelf text-to-image generation model, providing a solid foundation for a wide range of applications.

H. Effect of salient object matting model choice. How to extract high-quality alpha channels is critical for constructing high-quality single-layer transparent images. We study the influence of different salient object matting models, such as SAM2, BiRefNet, and RMBG-2.0, and summarize the comparison results on LAYER-BENCH in Table 8. We primarily consider the visual aesthetics of the transparent layers after matting and report the quantitative results. Additionally, we visualize the qualitative comparison results in Figure 15. We empirically find that RMBG-2.0 achieves the best results and adopt it as the default model.

I. Prompt of the Creative Caption Generation Compared to the common images in the MAGICK dataset, creative images reflect the model’s ability to generate less frequent and more novel visual content. To evaluate this capability of our method, we constructed a test set consisting of 500 creative prompts generated by GPT-4o, ensuring diversity and originality in the evaluation dataset. We mainly focus on single objective description generation

J. Prompt of Multi-layer Style-align Reception Instruction Given a reference layer of a multi-layer image, we leverage the visual recognition capabilities of GPT-4o and style-align reception instruction to transfer the original layer caption to a specific style caption. Specifically, we paste the original layer to the center of a gray background image while keeping the aspect ratio. Then, the style-specific instruction and the gray background layer image are fed to GPT-4o. Also, for the generation of ART, we use a similar instruction prompt to transfer the overall writing and style of the global caption.

K. How to choose the suffix prompt?

To understand how the suffix prompt helps the transparent layer generation task, we analyze the attention maps between the background regions and the color text tokens within the suffix prompt in Table 9, where we observe that the “gray” token achieves the best attention map response. We further conducted a series of experiments to compute mIoU_{FG} and mIoU_{BG} by calculating the mean IoU between the binary attention mask and the mask predicted by an image matting model to demonstrate the effect of choosing different suffix prompts quantitatively. In addition, we compute the mean square error between the attention map and the matting mask using MSE_{BG} and MSE_{FGLeak}, where the latter metric reflects the degree of information leakage from the background to the foreground regions. We

Method	Natural Object Layer Quality			Sticker Layer Quality			Creative Object Layer Quality		
	HPSv2 ↑	AE-V2.5 ↑	TIPS ↑	HPSv2 ↑	AE-V2.5 ↑	TIPS ↑	HPSv2 ↑	AE-V2.5 ↑	TIPS ↑
SAM2	26.24	5.374	30.03	26.04	4.556	24.49	<u>30.01</u>	5.251	<u>36.76</u>
BiRefNet	26.03	5.548	29.26	26.08	4.719	25.62	29.09	5.503	35.24
RMBG-2.0	26.58	5.617	30.19	26.14	4.735	25.69	29.55	5.551	36.25

Table 8: Effect of choosing different salient object matting models.



Figure 15: Qualitative comparison of different salient object matting models. From left to right, we show the matted results with RMBG-2.0, BiRefNet, and SAM2.

compute these metrics as follows:

$$\text{IoU}_{\text{BG}} = \frac{|(1 - \mathbf{M}) \cap \overline{\mathbf{A}}|}{|(1 - \mathbf{M}) \cup \overline{\mathbf{A}}|}, \quad \text{MSE}_{\text{BG}} = \frac{1}{N} \sum_{i=1}^N ((1 - \mathbf{M}_i) - \overline{\mathbf{A}}_i)^2, \quad (3)$$

$$\text{IoU}_{\text{FG}} = \frac{|\mathbf{M} \cap (1 - \overline{\mathbf{A}})|}{|\mathbf{M} \cup (1 - \overline{\mathbf{A}})|}, \quad \text{MSE}_{\text{FGLeak}} = \frac{1}{N} \sum_{i=1}^N (\mathbf{M}_i - \mathbf{M}_i \cdot \overline{\mathbf{A}}_i)^2, \quad (4)$$

where \mathbf{M} denotes the binary foreground mask predicted by a state-of-the-art image matting model, and $\overline{\mathbf{A}}$ denotes the binarized version of the attention mask \mathbf{A} computed between the suffix prompt tokens and the visual tokens extracted from the self-attention blocks within the diffusion transformer. N denotes the number of pixels. In addition, we also use a trajectory magnitude to analyze whether the diffusion model is able to control the background region pixels across all timesteps throughout the entire denoising trajectory.

Figure 9 visualizes the attention maps between the suffix tokens and the visual tokens. We can see that by choosing a suitable suffix prompt, we can elicit the potential of the diffusion transformer to generate isolated background regions that are easy to segment.

L. Effect of suffix prompt templates. As shown in Table 9, the design of the suffix prompt is important for guiding the text-to-image generation models to generate images consisting of objects that can be easily isolated from the background by ensuring an approximately single-colored background.

918 919 920 921 922 923 924 925 926 927 928 929 930	Suffix Prompt	Attention between Suffix text token and visual token				Trajectory Magnitude	
		mIoU _{BG} ↑	mIoU _{FG} ↑	MSE _{BG} ↓	MSE _{FGLeak} ↑	$\bar{d}_{FG} - \bar{d}_{BG}$ ↑	\bar{d}_{BG} ↓
		-	-	-	-	0.041	6.198
original (w/o background prompt)		-	-	-	-	0.041	6.198
half green and half red background		0.7863	0.5943	0.4717	0.2488	-0.202	6.427
half red and half blue background		0.7318	0.5403	0.4868	0.2413	-0.200	6.420
half gray and half black background		0.7902	0.5692	0.4478	0.2468	0.243	6.062
half gray and half white background		0.7787	0.5540	0.4701	0.2275	0.093	6.266
a solid red background		0.8282	0.6398	0.4414	0.2503	-1.412	7.814
a solid green background		0.8554	0.6646	0.4706	0.2401	-0.376	6.624
a solid blue background		0.8379	0.6493	0.4714	0.2416	-0.485	6.818
a solid black background		0.7318	0.5179	0.4255	0.2409	-1.749	8.317
a solid white background		0.8070	0.6495	0.3992	0.2365	-2.503	9.083
a solid transparent background		0.5801	0.3302	0.4410	0.2262	-1.413	7.872
a solid gray background		0.8642	0.6809	0.4181	0.2564	0.805	5.591

Table 9: Attention-map analysis of different suffix prompts.

933 934 935 936 937 938	Method	Natural Object Layer Quality			Sticker Layer Quality			Creative Object Layer Quality			Method	Natural Object Layer Quality			Sticker Layer Quality			Creative Object Layer Quality		
		HPSv2 ↑ AE-V2.5 ↑ TIPS ↑	HPSv2 ↑ AE-V2.5 ↑ TIPS ↑	HPSv2 ↑ AE-V2.5 ↑ TIPS ↑	HPSv2 ↑ AE-V2.5 ↑ TIPS ↑	HPSv2 ↑ AE-V2.5 ↑ TIPS ↑	HPSv2 ↑ AE-V2.5 ↑ TIPS ↑	HPSv2 ↑ AE-V2.5 ↑ TIPS ↑	HPSv2 ↑ AE-V2.5 ↑ TIPS ↑	HPSv2 ↑ AE-V2.5 ↑ TIPS ↑		Gray	26.58	5.617	30.19	26.14	4.735	25.69	29.55	5.551
SuffixPrompt A	26.13	5.609	29.83	26.07	4.758	25.67	29.12	5.572	36.25	Green	25.59	5.308	28.72	25.62	4.605	25.02	28.78	5.342	34.52	
SuffixPrompt B	26.29	5.587	29.95	25.98	4.726	25.45	29.28	5.529	36.32	Blue	26.29	5.434	29.53	25.83	4.690	25.63	29.29	5.456	35.55	
SuffixPrompt C	26.32	5.625	30.06	26.14	4.758	25.77	29.35	5.566	36.42	Red	25.70	5.267	28.40	25.68	4.618	25.49	28.72	5.400	34.46	
SuffixPrompt D	25.95	5.631	29.65	26.23	4.745	25.93	29.38	5.539	36.12	White	24.71	4.975	27.34	25.28	4.399	24.26	27.97	5.362	34.73	
SuffixPrompt E	26.07	5.493	29.35	26.12	4.739	25.76	28.78	5.497	34.84	Black	26.16	5.500	29.38	25.34	4.655	24.96	28.78	5.430	34.48	
SuffixPrompt F	26.01	5.607	29.43	26.10	4.755	25.75	29.28	5.518	35.70	Transparent	26.26	5.274	29.36	25.47	4.569	24.94	29.64	5.453	36.50	
SuffixPrompt G	26.45	5.468	30.07	25.72	4.654	25.30	29.87	5.397	36.14	Half red and half red	25.91	5.344	29.03	25.93	4.699	26.08	29.72	5.399	35.79	
SuffixPrompt H	26.58	5.617	30.19	26.14	4.735	25.69	29.55	5.551	36.25	Half red and half blue	25.83	5.418	29.10	25.99	4.691	26.05	29.75	5.459	35.89	

Table 10: Effect of choosing different suffix prompt templates.

Table 11: Effect of choosing different color within suffix prompt.

Here, we further compare the matting results of nine different suffix prompt designs in Table 10. We empirically find that choosing “*isolated on a solid gray background*” (SuffixPrompt H) achieves slightly better results.

M. Effect of color within suffix prompt. One natural question is which color is better for transparent layer generation. We investigate the influence of using different color words within the suffix prompt and summarize the results in Table 11. Accordingly, we find that using the color “gray” achieves the best results. This differs from the observation in previous work Burgert et al. (2024), which stated that using the color “green” performs best because “green” is the least common hue.

N. Photorealistic multi-layer image synthesis. In Figure 16, we adopt a top-down approach starting from the whole image generated by FLUX.1[dev] with synthetic object-driven prompts. Then, we train an anonymous object detector on our collected 800K multi-layer internal dataset to detect individual objects within the whole image. Following matting and inpainting, we obtain individual transparent layers and the background layer. After manual selection, we obtain 1K high-quality photo-realistic multi-layer images with accurate alpha mattes.

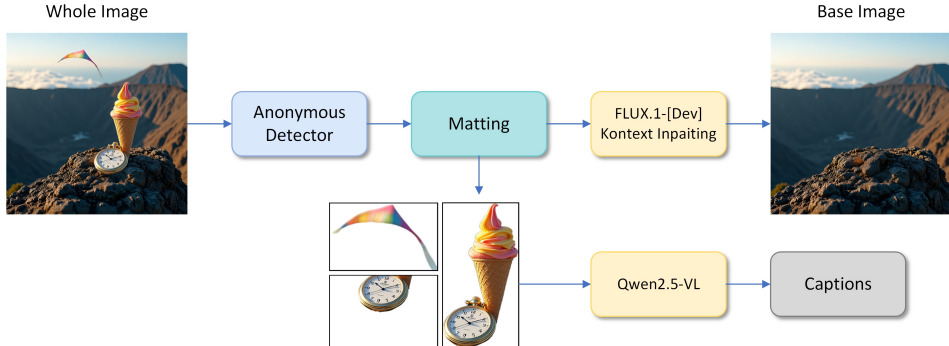
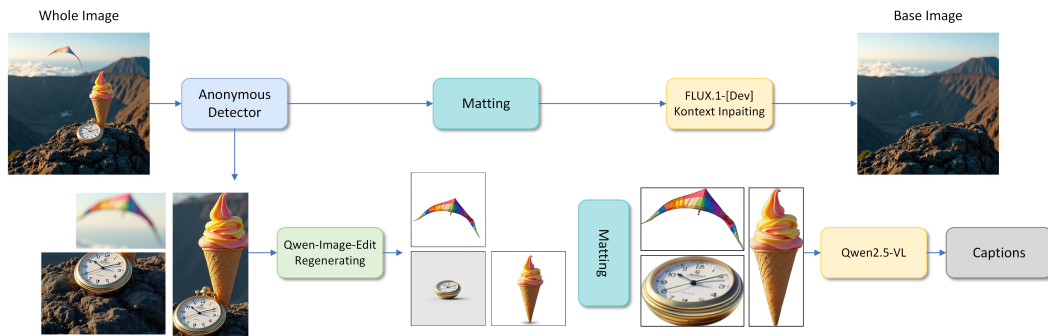


Figure 16: Photorealistic multi-layer data engine. Starting from a whole image generated by FLUX.1-[dev], we detect individual objects, and then leverage matting and inpainting to obtain individual transparent layers and the background layer.

972 **O. Qwen-Image Based Multi-layer Engine.** We further extent our method to Qwen-Image Wu
 973 et al. (2025), another state-of-the-art text-to-image generation model. As shown in Figure 21- 26, our
 974 method can also generate high-quality multi-layer transparent images based on Qwen-Image. We test
 975 first 50 images of the Japanese anime style split of PRISMLAYERSPRO, and the average TIPS score of
 976 all 491 layers of FLUX.1-[dev] and Qwen-Image are 22.53 and 23.45, respectively. Our TIPS model
 977 can effectively evaluate the quality of both text and object transparent layers.

978 **P. Advanced Photorealistic Multi-layer Data Engine.** As shown in Figure 17, we introduce our
 979 advanced photorealistic multi-layer data engine to further boost the performance of photorealistic
 980 multi-layer image generation. We mainly focus in improving the occlusion problem and physical
 981 consistency among different layers. We leverage Qwen-Image-Edit Wu et al. (2025) to regenerate the
 982 salient object in a blank background while keeping the original shape and details. By regenerating,
 983 we can overcome the occlusion problem and obtain high resolution layers with rich details while
 984 considering physical consistency.



985
 986 Figure 17: Advanced Photorealistic multi-layer data engine.
 987
 988

989 **Q. Analysis on Objects with Intrinsic Transparency** We conducted a dedicated evaluation focusing
 990 on the generation capabilities of our pipeline for objects with intrinsic transparency. We curated a list
 991 of 25 distinct object categories characterized by intrinsic transparency (e.g., glass marble, light bulb,
 992 ice cube). For each category, we leveraged Qwen3-VL-8B-Instruct Bai et al. (2025) to generate four
 993 distinct descriptive prompts, resulting in a total of 100 test prompts. We then utilized LayerFlux to
 994 generate the corresponding images in 1024×1024 resolution. For the segmentation, we evaluated two
 995 methods: RMBG-2.0 RMB and SAM 3 Carion et al. (2025). For SAM 3, the object category name
 996 was provided as the text prompt to guide the segmentation. Quantitative Evaluation: We assessed the
 997 quality of the segmented transparent regions using the TIPS (Transparency Information Performance
 998 Score) metric. We directly use the T2I prompt as the text description input to the TIPS model for
 999 evaluation. The evaluation was performed on the 100 generated samples.

1000
 1001 • RMBG-2.0 achieved an average TIPS score of 26.78.
 1002 • SAM 3 achieved an average TIPS score of 24.15.

1003 We provide all results and the corresponding prompts in the supplementary material. As shown in
 1004 Figure 18, we visualized the segmentation results. We observed that handling complex transparency
 1005 remains a challenging task for current state-of-the-art segmentation models. Specifically, both
 1006 RMBG-v2.0 and SAM 3 struggle to perfectly disentangle semi-transparent regions or accurately
 1007 recover fine-grained alpha values (opacity) in intricate areas. This limitation in high-fidelity alpha
 1008 matting for transparent objects is acknowledged as an open problem and remains a subject for future
 1009 work. However, despite these fine-grained limitations, our analysis demonstrates that for the majority
 1010 of cases, the models successfully identify and segment the complete object mask (isolating the object
 1011 from the background). This level of segmentation accuracy ensures that the generated assets are
 1012 sufficiently high-quality and usable for the construction of our dataset, maintaining the integrity of
 1013 the semantic layouts.

1014 **R. Overlapping Layers** In Figure 19, we present the statistics of overlapping layers in our PRISMLAY-
 1015 ERSPRO dataset. The average overlapping layer pair number is 6.32, indicating that our dataset contains
 1016 diverse and complex multi-layer structures. As shown in Figure 20, we provide some examples

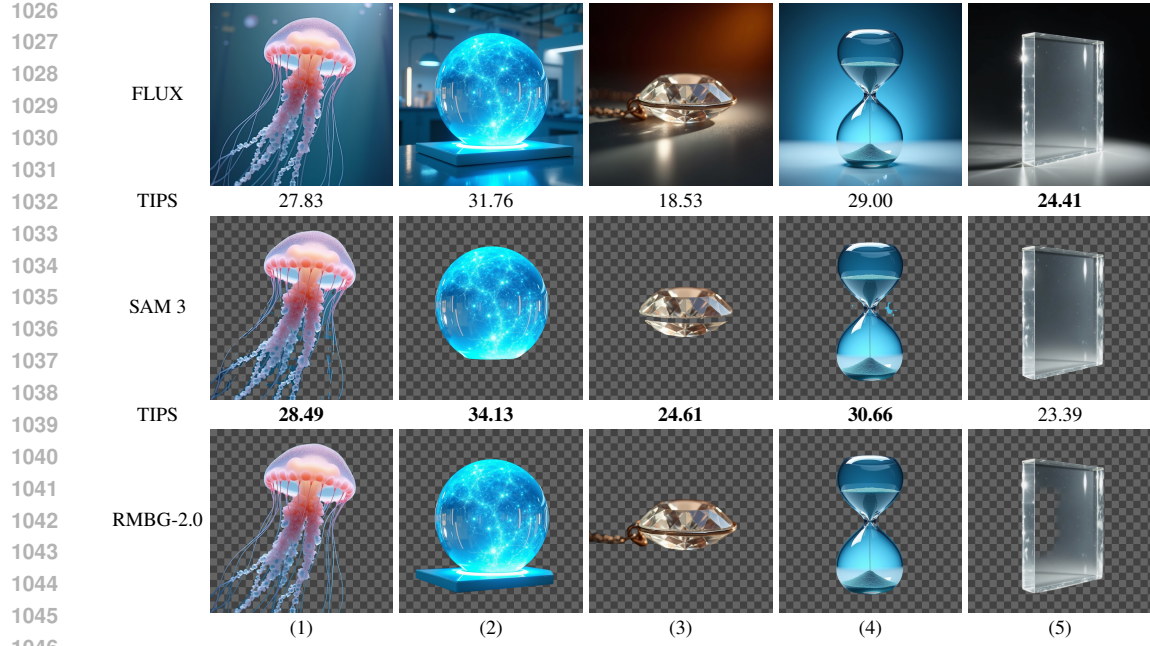


Figure 18: Qualitative comparison on objects with intrinsic transparency. From top to bottom, we show the generated image by FLUX.1-[dev], the segmentation results of SAM 3 and RMBG-2.0. The TIPS scores are shown below each result.

of overlapping layers in our **PRISM_LAYERS_PRO** dataset. We notice that the z-order of the layers is derived from real data and filtered by our proposed artifact detector and manual checking, ensuring the physical plausibility of our multi-layer images.

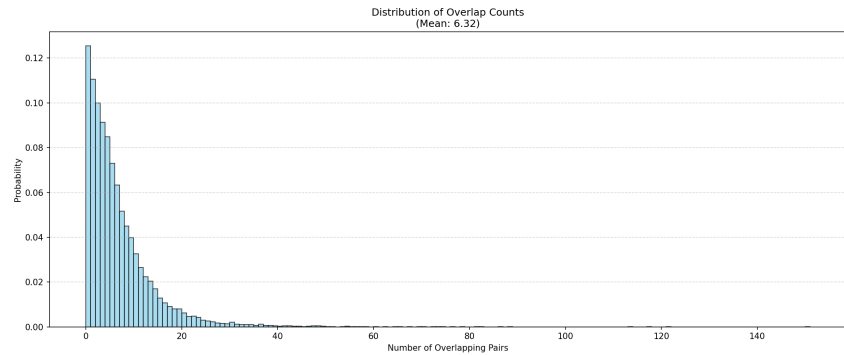
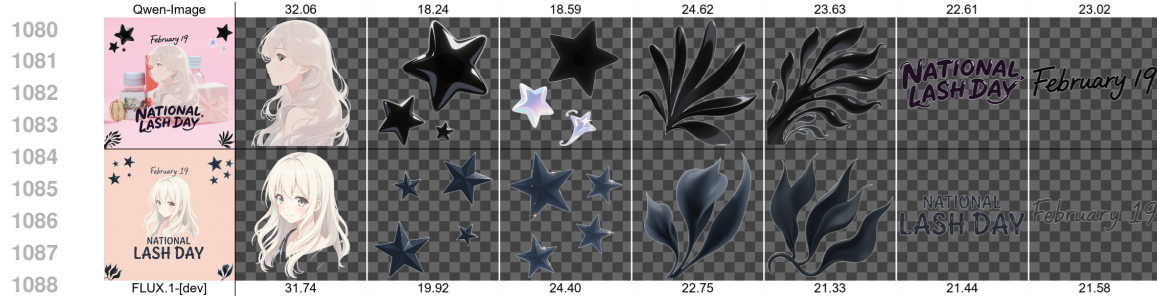


Figure 19: The statistics of overlapping layers in PRISM_LAYERS_{PRO}.



Figure 20: Examples of overlapping layers in our PRISM_LAYERS_{PRO} dataset.



(1) This is a Japanese anime style image. The illustration features flowing, wavy hair with soft, delicate lines. The hair is depicted in a light shade, with subtle highlights that suggest a glossy texture. The strands cascade elegantly, framing the face and creating a sense of movement. The overall composition conveys a gentle, serene vibe, typical of anime aesthetics, emphasizing beauty and grace in the hair's design, style: elegant, harmonious, sophisticated, isolated on a solid gray background.

(2) This is a Japanese anime style image. Text: None Three sparkling star shapes float gracefully, each varying in size and orientation. The largest star, with smooth, curvy edges, radiates a sense of whimsy, while the medium star has a slightly sharper silhouette, adding dynamic contrast. The smallest star, delicate and petite, completes the trio. Each star is a deep, rich black, exuding a glossy sheen that suggests a magical aura, enhancing the enchanting atmosphere of the composition, style: elegant, harmonious, sophisticated, isolated on a solid gray background.

(3) This is a Japanese anime style image. Three sparkling star shapes float gracefully, each varying in size and orientation. The largest star, a bold black silhouette, radiates a sense of mystery, while the medium star has a softer curve, suggesting a gentle twinkle. The smallest star, with a playful tilt, adds a whimsical touch. Their smooth, glossy surfaces reflect light, enhancing the enchanting atmosphere, reminiscent of magical moments in anime, style: elegant, harmonious, sophisticated, isolated on a solid gray background.

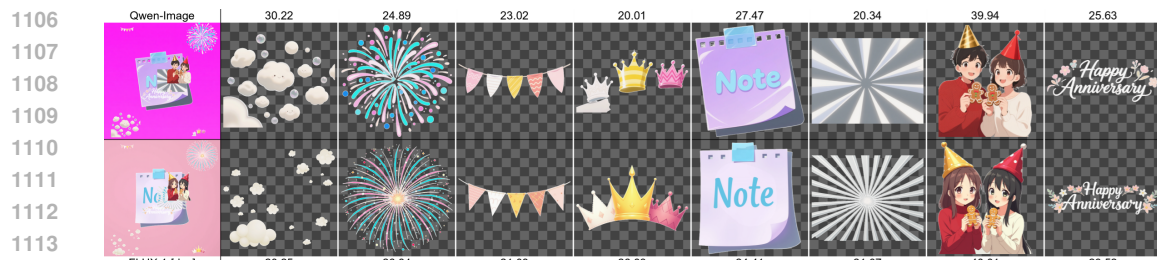
(4) This is a Japanese anime style image. The image features a dynamic arrangement of five stylized, elongated black shapes resembling fingers or petals, radiating outward from a corner. Each shape has a smooth, glossy texture, with subtle highlights that suggest a soft sheen. The forms vary in size and curvature, creating a sense of movement and flow, as if they are gently unfurling or reaching out, evoking a feeling of grace and elegance, style: elegant, harmonious, sophisticated, isolated on a solid gray background.

(5) This is a Japanese anime style image. The composition features a series of stylized, black, organic shapes resembling flowing, elongated fingers or petals. Each shape has a smooth, glossy texture, with subtle gradients that suggest depth and curvature. The arrangement creates a dynamic sense of movement, as if the forms are gently reaching outward, inviting the viewer into a whimsical, fantastical realm. The interplay of light and shadow enhances the overall elegance of the design, style: elegant, harmonious, sophisticated, isolated on a solid gray background.

(6) Text: 'NATIONAL LASH DAY' in a playful, curved font, featuring bold, dark letters with a slight glossy sheen, reminiscent of a whimsical anime title. The letters are slightly uneven, adding a charming, hand-drawn quality, evoking a sense of celebration and joy, style: elegant, harmonious, sophisticated, isolated on a solid gray background.

(7) Text: 'February 19' in playful, handwritten black script with a slight tilt, evoking a sense of whimsy and charm, reminiscent of a light-hearted Japanese anime scene, style: elegant, harmonious, sophisticated, isolated on a solid gray background.

Figure 21: Qualitative comparison of multi-layer transparent image generation based on Qwen-Image and FLUX.1-[dev]. The TIPS scores are shown above and below each layer.



(1) This is a Japanese anime style image. The foreground features a whimsical scattering of soft, rounded shapes in varying sizes, resembling delicate, fluffy clouds or playful bubbles. Each shape is a gentle off-white, with subtle shading that gives them a three-dimensional appearance. The arrangement is random yet harmonious, creating a sense of lightness and joy, as if they are floating in a serene, dreamlike atmosphere, style: elegant, harmonious, sophisticated, isolated on a solid gray background.

(2) This is a Japanese anime style image. Text: None A vibrant explosion of color radiates outward, featuring delicate, swirling lines in bright turquoise and soft pink. The lines, resembling fireworks, are adorned with small, circular accents in varying shades of blue and pink, creating a whimsical, dynamic effect. The intricate layering of the lines suggests movement, as if the fireworks are bursting into life, illuminating the scene with a playful, enchanting energy, style: elegant, harmonious, sophisticated, isolated on a solid gray background.

(3) This is a Japanese anime style image. A whimsical string of five colorful triangular flags flutters gently, each adorned with unique patterns. The first flag is a soft pink with delicate zigzag lines, followed by a white flag featuring subtle stripes. Next, a vibrant yellow flag stands out with bold diagonal lines, while a coral flag showcases a playful wavy design. The final flag is a light pastel pink, completing the cheerful display, style: elegant, harmonious, sophisticated, isolated on a solid gray background.

(4) This is a Japanese anime style image. Three whimsical crowns rise playfully along a curved horizon. The leftmost crown is a soft white with delicate, wavy patterns, while the center crown shines in a bright yellow, adorned with bold, horizontal stripes. The rightmost crown is a vibrant pink, featuring intricate zigzag designs. Each crown has a slight sheen, suggesting a magical aura, and they are layered in a way that creates a sense of depth and movement, style: elegant, harmonious, sophisticated, isolated on a solid gray background.

(5) This is a Japanese anime style image. Text: 'Note' in playful, rounded, pastel blue lettering with a soft shadow effect. A large, lavender square note paper dominates the scene, featuring a glossy texture that catches light. At the top, a translucent, sky-blue tape holds the note, adding a whimsical touch. The note's edges are slightly curled, suggesting a gentle breeze, while small, square cutouts along the top create a charming, decorative border, style: elegant, harmonious, sophisticated, isolated on a solid gray background.

(6) This is a Japanese anime style image. Text: None. The image features a dynamic arrangement of elongated, angular lines radiating outward, resembling sun rays. Each line is a soft white, with subtle gradients that suggest depth. The varying thicknesses create a sense of movement, as if the rays are bursting forth. The interplay of light and shadow adds a delicate texture, enhancing the overall energetic feel of the composition, style: elegant, harmonious, sophisticated, isolated on a solid gray background.

(7) This is a Japanese anime style image. The scene features two individuals wearing festive party hats shaped like cones, one in gold and the other in a vibrant red. They hold gingerbread cookies shaped like cheerful figures, with intricate icing details. The textures of their clothing, a cozy red sweater and a soft white top, contrast beautifully. The warm colors and playful expressions evoke a joyful celebration, enhanced by the whimsical atmosphere typical of anime, style: elegant, harmonious, sophisticated, isolated on a solid gray background.

(8) Text: 'Happy Anniversary' in elegant, flowing white script with a soft, shimmering effect, surrounded by delicate pastel-colored floral motifs that evoke a sense of celebration and warmth. The letters appear to dance lightly, as if caught in a gentle breeze, enhancing the joyful atmosphere of the occasion, style: elegant, harmonious, sophisticated, isolated on a solid gray background.

Figure 22: Qualitative comparison of multi-layer transparent image generation based on Qwen-Image and FLUX.1-[dev]. The TIPS scores are shown above and below each layer.



(1) This is a Japanese anime style image. A young woman with flowing, wavy hair, dressed in a cozy, oversized beige sweater, gestures with her right hand, palm up, as if inviting conversation. The soft texture of her sweater contrasts with the smooth, light wood paneling in the background. A stylish white lamp stands nearby, casting a warm glow, enhancing the inviting atmosphere of the scene, style: elegant, harmonious, sophisticated, isolated on a solid gray background.

(2) Text: 'Happy Women's Day' in elegant, flowing cursive with a shimmering golden hue, each letter adorned with delicate highlights that evoke a sense of warmth and celebration, reminiscent of a gentle breeze in a serene anime landscape. The letters dance gracefully, embodying the spirit of joy and empowerment, inviting all to partake in the festivities of this special day, style: elegant, harmonious, sophisticated, isolated on a solid gray background.

(3) Text: 'Just wanted you to know that you're the coolest, strongest, and most amazing woman in the world.' in elegant, flowing cursive with a soft golden hue, each letter shimmering as if kissed by starlight, surrounded by delicate sparkles that evoke a sense of warmth and admiration, reminiscent of heartfelt messages in a Japanese anime scene, style: elegant, harmonious, sophisticated, isolated on a solid gray background.

(4) This is a Japanese anime style image. The image features a long, narrow strip of soft, creamy beige fabric with a slightly frayed edge, suggesting a delicate texture. The fabric appears to have a subtle sheen, reflecting light gently, enhancing its ethereal quality. The strip is positioned horizontally, evoking a sense of calm and simplicity, reminiscent of traditional Japanese textiles, with a serene and understated elegance, style: elegant, harmonious, sophisticated, isolated on a solid gray background.

(5) Text: 'Hey, sis!' in elegant, flowing cursive with a warm, bronze hue, featuring a soft, shimmering effect that gives it a three-dimensional appearance, as if the letters are gently rising from the surface. The text is slightly tilted, adding a playful dynamic, and the subtle highlights enhance its charm, reminiscent of a whimsical Japanese anime aesthetic, style: elegant, harmonious, sophisticated, isolated on a solid gray background.

(6) This is a Japanese anime style image. The delicate flower features five translucent white petals, each with soft, rounded edges and a subtle sheen that catches the light. The petals are adorned with faint yellow and brown accents near the base, creating a gentle gradient. At the center, a rich, dark brown cluster of stamens radiates outward, adding depth and contrast. The overall composition exudes a serene, ethereal beauty, reminiscent of a tranquil anime garden scene, style: elegant, harmonious, sophisticated, isolated on a solid gray background.

(7) This is a Japanese anime style image. A delicate flower with five soft, creamy white petals radiates outward, each petal slightly curled at the edges, showcasing a subtle sheen. The center is a rich, dark brown, densely packed with tiny, intricate stamens, creating a striking contrast. The petals exhibit gentle gradients, hinting at a whisper of yellow near the base, enhancing their ethereal beauty. The overall composition evokes a sense of tranquility and grace, style: elegant, harmonious, sophisticated, isolated on a solid gray background.

(8) This is a Japanese anime style image. A slender, delicate branch stretches vertically, adorned with vibrant, fluffy yellow pom-pom flowers that resemble miniature suns. Each flower is a bright, cheerful yellow, with soft, feathery textures that catch the light, creating a gentle glow. The thin, slightly twisted stem is a muted brown, adding a natural contrast to the vivid blossoms, evoking a sense of serene beauty and whimsy, style: elegant, harmonious, sophisticated, isolated on a solid gray background.

(9) This is a Japanese anime style image. A delicate, crumpled strip of pale cream paper lies at an angle, its soft texture resembling silk. Subtle shadows accentuate its folds, creating a sense of depth. The edges are slightly frayed, hinting at gentle wear. The light catches the surface, giving it a faint sheen, while the overall composition evokes a serene, minimalist aesthetic typical of anime art, style: elegant, harmonious, sophisticated, isolated on a solid gray background.

Figure 23: Qualitative comparison of multi-layer transparent image generation based on Qwen-Image and FLUX.1-[dev]. The TIPS scores are shown above and below each layer.



(1) This is a Japanese anime style image. The design features two elongated, parallel lines that gracefully extend vertically, converging at a central, symmetrical oval shape. The lines are outlined in a deep, rich brown, evoking a sense of elegance. The oval, nestled between the lines, adds a touch of softness, creating a harmonious balance. The overall composition suggests a serene, minimalist aesthetic, reminiscent of traditional Japanese art forms, style: elegant, harmonious, sophisticated, isolated on a solid gray background.

(2) This is a Japanese anime style image. The design features two elongated, parallel lines that gracefully converge at the center, forming a delicate, symmetrical shape reminiscent of an hourglass. The lines are outlined in a soft, dark hue, creating a subtle contrast against the background. The central shape, an elegant oval, adds a sense of harmony and balance, evoking a feeling of tranquility and fluidity in its minimalist elegance, style: elegant, harmonious, sophisticated, isolated on a solid gray background.

(3) This is a Japanese anime style image. The character wears a red and white checkered shirt, with soft, flowing hair cascading down her shoulders. Her arms are outstretched, palms up, suggesting a welcoming gesture. The shirt's fabric appears textured, with subtle shading enhancing its folds. The overall composition conveys a sense of openness and curiosity, embodying the vibrant and expressive nature typical of anime art, style: elegant, harmonious, sophisticated, isolated on a solid gray background.

(4) This is a Japanese anime style image. A perfectly round, deep black circle dominates the scene, exuding an aura of mystery and elegance. The surface appears smooth and glossy, reflecting subtle hints of light that create a soft sheen. The edges are sharply defined, enhancing the contrast against the surrounding space, while the overall simplicity invites intrigue, reminiscent of a portal to another world in a fantastical anime setting, style: elegant, harmonious, sophisticated, isolated on a solid gray background.

(5) This is a Japanese anime style image. A large, perfectly round shape fills the frame, rendered in a deep, rich black hue. The surface appears smooth and glossy, reflecting subtle highlights that suggest a soft sheen. The edges are sharply defined, creating a striking contrast against the surrounding space, evoking a sense of depth and dimensionality, as if the circle is floating in an ethereal realm, style: elegant, harmonious, sophisticated, isolated on a solid gray background.

(6) Text: 'CHOOSE YOUR FAVORITE CLASS!' in bold, elegant black lettering with a slight glossy sheen, exuding a sense of adventure and excitement, reminiscent of a vibrant anime world where choices lead to epic journeys, style: elegant, harmonious, sophisticated, isolated on a solid gray background.

(7) Text: 'Exercise Edition' in elegant, slender, dark maroon lettering, exuding a soft, refined aura, reminiscent of a serene Japanese calligraphy style, style: elegant, harmonious, sophisticated, isolated on a solid gray background.

(8) Text: 'Zumba' in soft pink, elegant font, 'Dance' in the same delicate style, and 'Boxing' in matching pastel pink, all aligned vertically with a gentle, flowing rhythm, evoking a sense of movement and energy, reminiscent of a lively anime dance scene, style: elegant, harmonious, sophisticated, isolated on a solid gray background.

(9) Text: 'Pilates' in soft pink, elegant, rounded font, and 'Yoga' in matching soft pink, slightly larger, both exuding a calming, serene aura reminiscent of gentle cherry blossoms in spring, style: elegant, harmonious, sophisticated, isolated on a solid gray background.

Figure 24: Qualitative comparison of multi-layer transparent image generation based on Qwen-Image and FLUX.1-[dev]. The TIPS scores are shown above and below each layer.

1188

1189

1190

1191

1192

1193

1194

1195

1196

1197

1198

1199

1200

1201

1202

1203

1204

1205

1206

1207

1208

1209

1210

1211

1212

1213

1214

1215

1216

1217

1218

1219

1220

1221

1222

1223

1224

1225

1226

1227

1228

1229

1230

1231

1232

1233

1234

1235

1236

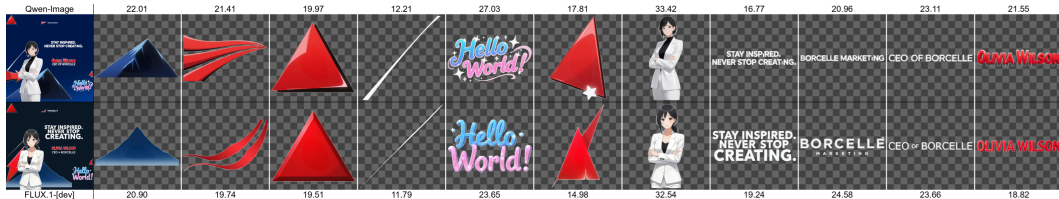
1237

1238

1239

1240

1241



(1) This is a Japanese anime style image. The image features a large, dark blue triangular shape, resembling a stylized roof or mountain peak. The edges are sharply defined, creating a bold silhouette. The surface has a smooth texture, reflecting light subtly, enhancing its dimensionality. The overall composition conveys a sense of stability and strength, with the triangular form suggesting upward movement, evoking feelings of aspiration and adventure, style: elegant, harmonious, sophisticated, isolated on a solid gray background.

(2) This is a Japanese anime style image. Three sleek, elongated red stripes curve gracefully, each one slightly overlapping the next. The vibrant red hue is accentuated by a subtle black outline, giving the shapes a bold, dynamic appearance. The stripes taper at one end, suggesting a sense of motion, as if they are flowing or being swept by a gentle breeze, embodying a sense of energy and fluidity, style: elegant, harmonious, sophisticated, isolated on a solid gray background.

(3) This is a Japanese anime style image. A vibrant red triangle dominates the composition, its sharp edges contrasting against a subtle black outline that adds depth. The surface of the triangle exhibits a smooth texture, reflecting light in a way that suggests a glossy finish. The bold color evokes a sense of energy and passion, while the geometric simplicity creates a striking visual impact, reminiscent of dynamic anime aesthetics, style: elegant, harmonious, sophisticated, isolated on a solid gray background.

(4) This is a Japanese anime style image. The image features a single, slender white line that diagonally traverses the canvas, creating a sense of dynamic movement. The line is smooth and sharp, with a slight glow that suggests an ethereal quality. Its placement draws the eye across the space, evoking a feeling of tension and elegance, reminiscent of minimalist anime aesthetics, style: elegant, harmonious, sophisticated, isolated on a solid gray background.

(5) This is a Japanese anime style image. Text: 'Hello World!' in vibrant, swirling blue and pink letters, adorned with sparkling stars and a soft, ethereal glow, creating a whimsical and inviting atmosphere. The letters are playfully arranged, with the 'H' and 'W' slightly larger, giving a dynamic feel, as if they are dancing across the canvas, inviting viewers into a magical realm, style: elegant, harmonious, sophisticated, isolated on a solid gray background.

(6) This is a Japanese anime style image. A vibrant red triangle, sharply pointed to the left, dominates the scene. Its edges are outlined in a thin, dark line, enhancing its boldness. The surface of the triangle has a smooth texture, reflecting light subtly, giving it a slightly glossy appearance. A small white star glimmers at the base, adding a touch of whimsy and charm to the overall composition, style: elegant, harmonious, sophisticated, isolated on a solid gray background.

(7) This is a Japanese anime style image. The figure is dressed in a sleek, tailored white blazer, exuding an air of confidence. The fabric appears smooth with subtle highlights, reflecting light elegantly. The blazer is complemented by a black top underneath, creating a striking contrast. The arms are crossed, suggesting a poised demeanor. The overall composition conveys a sense of professionalism and strength, enhanced by the clean lines and polished appearance of the attire, style: elegant, harmonious, sophisticated, isolated on a solid gray background.

(8) Text: "STAY INSPIRED. NEVER STOP CREATING." in large, bold, white lettering with a soft, ethereal glow, reminiscent of a magical aura, embodying the spirit of creativity and motivation in a vibrant, anime-inspired style, style: elegant, harmonious, sophisticated, isolated on a solid gray background.

(9) Text: 'BORCELLE MARKETING' in sleek, modern sans-serif font, with a crisp white color that stands out prominently, evoking a sense of professionalism and clarity. The letters are evenly spaced, creating a balanced composition that draws the eye effortlessly across the text. The overall aesthetic is clean and minimalist, embodying a contemporary design that resonates with the themes of innovation and efficiency, reminiscent of a Japanese anime style, style: elegant, harmonious, sophisticated, isolated on a solid gray background.

(10) Text: 'CEO OF BORCELLE' in sleek, modern, sans-serif white lettering, exuding a professional aura, with a subtle shadow effect that adds depth, reminiscent of a high-tech corporate environment in a Japanese anime style, style: elegant, harmonious, sophisticated, isolated on a solid gray background.

(11) Text: 'OLIVIA WILSON' in bold, vibrant red lettering with a slight 3D effect, giving it a dynamic presence. The letters are sharply defined, with a glossy finish that reflects light, enhancing their prominence. The overall composition exudes a sense of energy and style, reminiscent of a character nameplate in a Japanese anime series, capturing attention with its striking color and bold typography, style: elegant, harmonious, sophisticated, isolated on a solid gray background.

Figure 25: Qualitative comparison of multi-layer transparent image generation based on Qwen-Image and FLUX.1-[dev]. The TIPS scores are shown above and below each layer.

1242

1243

1244

1245

1246

1247

1248

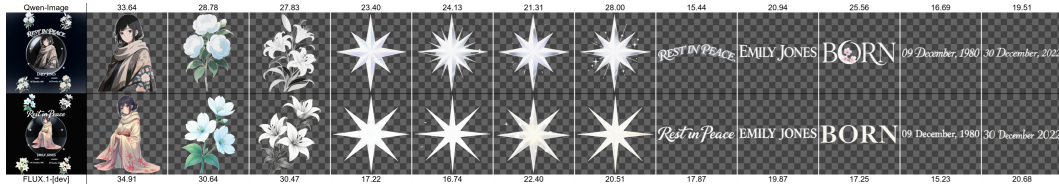
1249

1250

1251

1252

1253



(1) This is a Japanese anime style image. The figure is adorned in a richly patterned shawl featuring delicate floral motifs in soft pastels, contrasting with the deep shadows around. The intricate textures of the fabric suggest warmth and comfort. A flowing scarf wraps around the neck, cascading down with gentle folds, while the overall composition evokes a sense of mystery and depth, enhanced by the elegant arch framing the figure, style: elegant, harmonious, sophisticated, isolated on a solid gray background.

(2) This is a Japanese anime style image. Text: None. Delicate, large blossoms with rounded petals in soft shades of white and pale blue, intricately detailed with fine lines. The flowers are adorned with subtle highlights, giving them a gentle glow. Graceful green leaves with intricate veins cascade alongside, enhancing the floral arrangement's elegance. A slender stem supports the blooms, creating a harmonious flow, evoking a sense of serene beauty and tranquility typical of anime aesthetics, style: elegant, harmonious, sophisticated, isolated on a solid gray background.

(3) This is a Japanese anime style image. Text: None. The artwork features a delicate arrangement of elegant lilies, their petals intricately detailed with soft curves and sharp edges. The flowers are depicted in a monochromatic scheme, showcasing a blend of smooth and textured surfaces. Wispy leaves intertwine gracefully, enhancing the composition's fluidity. The overall design exudes a serene beauty, reminiscent of traditional Japanese art, with a focus on harmony and natural elegance, style: elegant, harmonious, sophisticated, isolated on a solid gray background.

(4) This is a Japanese anime style image. A radiant, eight-pointed star glimmers at the center, its sharp, elongated points radiating outward. The star is a brilliant white, with a soft, ethereal glow that creates a shimmering effect around its edges. Subtle gradients of light and shadow enhance its three-dimensional appearance, giving it a magical, otherworldly quality, reminiscent of celestial phenomena in anime, style: elegant, harmonious, sophisticated, isolated on a solid gray background.

(5) This is a Japanese anime style image. A radiant starburst glimmers at the center, featuring sharp, elongated points that radiate outward. The star is a brilliant white, with a soft, ethereal glow that creates a shimmering effect. Each point is delicately outlined in a subtle silver hue, enhancing its luminous quality. The interplay of light and shadow gives the star depth, evoking a sense of magic and wonder, style: elegant, harmonious, sophisticated, isolated on a solid gray background.

(6) This is a Japanese anime style image. A radiant, eight-pointed star glimmers with a soft, ethereal glow at its center, surrounded by delicate shimmering rays that extend outward. The star's points are sharp and elongated, each adorned with a subtle gradient from bright white at the core to a gentle silver at the tips, creating a mesmerizing effect. The overall composition evokes a sense of magic and wonder, reminiscent of celestial themes in anime, style: elegant, harmonious, sophisticated, isolated on a solid gray background.

(7) This is a Japanese anime style image. A radiant starburst glimmers at the center, featuring sharp, elongated points that radiate outward. The star is a brilliant white, with soft gradients transitioning to a delicate silver at the tips. Subtle sparkles surround it, enhancing its ethereal glow. The overall effect is one of magical luminescence, evoking a sense of wonder and enchantment, typical of anime aesthetics, style: elegant, harmonious, sophisticated, isolated on a solid gray background.

(8) Text: 'REST IN PEACE' in elegant, flowing white lettering, arched gracefully, reminiscent of a serene memorial. The font features soft curves and sharp edges, embodying a tranquil yet poignant atmosphere, enhanced by a subtle shadow that adds depth and dimension. The overall composition evokes a sense of calm and reflection, perfectly suited for a Japanese anime style, where emotions are conveyed through delicate artistry, style: elegant, harmonious, sophisticated, isolated on a solid gray background.

(9) Text: 'EMILY JONES' in large, bold, elegant white lettering with a soft, ethereal glow, reminiscent of a magical aura, embodying a serene and enchanting atmosphere typical of Japanese anime, style: elegant, harmonious, sophisticated, isolated on a solid gray background.

(10) Text: 'BORN' in elegant, slender, white lettering with a soft, ethereal glow, reminiscent of moonlight filtering through cherry blossoms, embodying a sense of new beginnings and hope, style: elegant, harmonious, sophisticated, isolated on a solid gray background.

(11) Text: '09 December, 1980' in elegant, soft white lettering with a delicate, shimmering effect, reminiscent of moonlight, evoking a sense of nostalgia and tranquility. The characters are gracefully spaced, with a slight curve that adds a whimsical touch, embodying the charm of Japanese anime aesthetics, style: elegant, harmonious, sophisticated, isolated on a solid gray background.

(12) Text: '30 December, 2022' in elegant, soft white lettering with a delicate, shimmering effect, reminiscent of moonlight reflecting on water, embodying a serene and tranquil atmosphere typical of Japanese anime aesthetics, style: elegant, harmonious, sophisticated, isolated on a solid gray background.

1282 Figure 26: Qualitative comparison of multi-layer transparent image generation based on Qwen-Image and 1283 FLUX.1-[dev]. The TIPS scores are shown above and below each layer.

1284

1285

1286

1287

1288

1289

1290

1291

1292

1293

1294

1295

1296
1297**Text Sticker Reception Prompt for GPT-4o**

1298

You are given the key word of a text sticker and its corresponding image. Your task is to generate an accurate and descriptive caption for the sticker, following these guidelines:

1299

1. The caption begins with "The text sticker describes/contains/" and ends with "isolated on a solid transparent background."
2. Clearly describe the text in the sticker, including the font color, font style, and any visual effects (e.g., shadows, gradients) observed in the image.

1300

3. Keywords usually refer to the text in the sticker, and you may include other relevant descriptive elements. Be explicit about these in your caption.

1301

4. Refer to the examples provided for clarity on how to construct your caption. Aim for creativity while adhering to the required structure.

1302

Here are some examples for reference:

1303

- "The text sticker presents the word 'Focus' in a sharp, modern font, filled with a gradient of charcoal gray to bright red. The letters are outlined in bright white, and stylized targets surround the text, conveying determination and clarity, isolated on a solid transparent background."

1304

- "The text sticker showcases the word 'Celebrate' in a festive, curly font, filled with a vibrant confetti gradient of rainbow colors. Each letter is dotted with tiny sparkles, and balloons and streamers float around, enhancing the joyful spirit of celebration, isolated on a solid transparent background."

1305

Please ensure to generate a caption that fits this style and adheres to the guidelines.

1306

1307

Response 1:

1308

{response 1}

1309

1310

Please strictly follow the following format requirements when outputting, and don't have any other unnecessary words.

1311

Output Format:

1312

response 1 or response 2.

1313

1314

1315

1316

1317

Creative Object Layer Prompt for GPT-4o

1318

You are tasked with generating imaginative and creative image descriptions based on a given object word. The generated description should follow these specific guidelines:

1319

1. Input:

1320

- You will receive a single object word (e.g., "penguin", "teapot", "robot", etc.).

1321

- Use this object as the central focus of the description.

1322

2. Output Requirements:

1323

- The description should be **creative and unexpected**, modifying the object or adding elements that make it unusual, humorous, or visually striking.

1324

- The description **must not include details about the background**—focus only on the main object and any additional elements that make it more interesting.

1325

- Aim for a **concise but vivid** description, ideally **within 20 to 30 words**.

1326

- Use **strong visual language** to create a mental image.

1327

- Avoid generic descriptions—make it **fun, unique, and imaginative**.

3. Examples for Reference:

1328

Given Object	Generated Description
--------------	-----------------------

1329

Kangaroo	A kangaroo holding a beer, wearing ski goggles and passionately singing silly songs.
----------	--

1330

Car	A car made out of vegetables.
-----	-------------------------------

1331

Raccoon	A cyberpunk-styled raccoon wearing neon glasses and a futuristic jacket, holding a laser gun in one paw.
---------	--

1332

Teapot	A giant teapot with robotic arms, serving tea while wearing a tiny monocle and top hat.
--------	---

1333

Penguin	A punk-styled penguin with a mohawk, leather jacket, and electric guitar, rocking out on an ice stage.
---------	--

1334

4. Constraints & Guidelines:

1335

- Do **not** include the background in the description.

1336

- Feel free to **modify the object's appearance, abilities, or accessories** to make it more interesting.

1337

- If necessary, **add related objects** (e.g., a robot might have futuristic gadgets, a dog might have sunglasses and a skateboard).

1338

- Keep the tone fun, artistic, and engaging.

1339

5. Additional Notes:

1340

Please directly respond to the prompt with the creative description.

1341

1342

1343

1344

1345

1346

1347

1348

1349

1350
1351**Multi-layer Style Reception Instruction for GPT-4o**1352
1353

You will receive an RGBA image placed on a gray background. Your task is to generate a highly detailed description of the image's content while adhering to a given stylistic (STYLEPROMPT) requirement.

Key Guidelines:

1. **Ignore the Gray Background:** - Do not mention or describe the gray background in any way. Focus solely on the foreground content.
2. **Handling Text in the Image:** - If the image contains any textual elements, the description **must** begin with **"Text:"** followed by a precise transcription of all visible text. - Transcribe every word, symbol, punctuation mark, and character **without omission or modification**. - The description of text must be brief and the style description should be limited to 5 words.
3. **Handling Non-Text Elements:** - If the image contains **non-text elements**, generate an **detailed** description, capturing all visible aspects. - Ensure that the provided style, STYLEPROMPT, is seamlessly **integrated** into the description, maintaining coherence and natural flow.
4. **Output Format:** - Provide only the description of the image. Do **not** include any additional explanations, comments, or meta-information about the task itself. - The description **must explicitly state** that the image is in **STYLEPROMPT style**, starting with **"This is a STYLEPROMPT style image."** (VERY IMPORTANT) - Limited to 70 words!!!

The image is shown below:

1362

1363

1364

1365

1366

1367

1368

1369

1370

1371

1372

1373

1374

1375

1376

1377

1378

1379

1380

1381

1382

1383

1384

1385

1386

1387

1388

1389

1390

1391

1392

1393

1394

1395

1396

1397

1398

1399

1400

1401

1402

1403